약학박사학위논문

암 유래 osteopontin 의 암 면역억제 작용기전 및 변형 adenovirus 를 이용한 B 세포백신의 향상된 항암효과 연구

Tumor immune suppression mechanism of tumor-derived osteopontin and enhanced antitumor immunotherapeutic effect of B cell-based vaccine transduced with modified adenoviral vector

2014년 2월

서울대학교 대학원

약학과 의약생명과학 전공

김 은 경

Abstract

Tumor immune suppression mechanism of tumor-derived osteopontin and enhanced antitumor immunotherapeutic effect of B cell-based vaccine transduced with modified adenoviral vector

Kim, Eun-Kyung

Laboratory of Immunology

Pharmaceutical Bioscience

Department of Pharmacy

The Graduate School

Seoul National University

Breaking the tumor-derived immunosuppressive environment and initiating strong immune responses against tumor antigens are both necessary for eliminate established tumors. Therefore, we investigated mechanisms of tumor-derived immunosuppression and attempted to develop more effective B cell based vaccine. These two different strategies were described in different sections respectively part I and part II.

Tumor cells secrete soluble factors to suppress host immunity against tumor for

improvement of their survival. Expansion of myeloid derived suppressor cells (MDSCs) is one of host immune suppression mechanism derived by tumors. Extramedullary myelopoiesis has been known as a common phenomenon in the tumor bearing hosts, which cause abnormal myeloid cell expansion in the peripheral lymphoid organ and tumor site. Although it is assumed that inflammatory mediators contribute to tumor-induced extramedullary myelopoiesis, responsible factor and its contribution remains still elusive. Using cytokine array, we found that osteopontin was increased in both spleen lysates and sera in the tumor bearing mice. Based on this, we investigated whether tumor-derived osteopontin affect extramedullary myelopoiesis and MDSC accumulation in the tumor environment. Knock down and neutralizing of osteopontin in the tumor cells showed reduced tumor growth, splenomegaly and extramedullary myelopoiesis in the tumor bearing mice. In the primary cultured splenocytes, osteopontin increased the proliferation of lineage^{neg}/CD127^{-}/CD117^{+}/Sca1^{-} heterogeneous myeloid progenitor populations (LK cells). Moreover, osteopontin increased migration of bone marrow LK cells. These results suggest that osteopontin induced increased extramedullary myelopoiesis and subsequently accumulated immunosuppressive MDSCs. Taken together, these findings suggested that osteopontin could become therapeutic target to overcome tumor-derived immunosuppressive environment.

For successful clinical tumor immunotherapy outcomes, strong immune responses against tumor antigens must be generated. Cell based vaccines

compromise one strategy with which to induce appropriate strong immune responses. Previously we established a natural killer T cell (NKT) ligand loaded and Her2/*neu* introduced modified adenoviral vector (Ad-k35HM) transduced-B cell based anticancer cellular vaccine. An Ad-k35HM transduced B cell vaccine elicited strong antigen specific cellular and humoral immune responses, subsequently showed inhibition of the *in vivo* growth of established tumors in a mouse model. In this study, we additionally investigated diverse characteristics of Ad-k35HM introduced B cell-based vaccine. Furthermore, the vaccine elicited HLA-A2 epitope specific cytotoxic T cell responses in B6.Cg (CB)-Tg (HLA-A/H2-D) 2Enge/Jat mice (AAD mice). These findings indicated that the Ad-k35 could be appropriate for the preclinical and clinical development of B cell-based anticancer immunotherapies.

Keywords: Myeloid derived suppressor cells (MDSC), Extramedullary myelopoiesis, Osteopontin, Myeloid progenitor cells (lineage^{neg}/CD127^{-} /CD117^{+}/Sca1^{-}, LK cells). B cell-based vaccine, AAD mice

Student number: 2009-30459

Table of Contents

List of Figures

Part I. Tumor-derived osteopontin act as an immune suppressor factor through accumulating myeloid-derived suppressor cells (MDSCs)

Part II. Enhanced antitumor immunotherapeutic effect of B cell-based vaccine transduced with modified adenoviral vector containing type 35 fiber structures

Abbreviations

Ab, antibody

Ag, antigen

APC, antigen presenting cell

ARG1, arginase 1

BrdU, bromodeoxyuridine

CD, cluster of differentiation

CFSE, 5-(and-6) carboxyfluorescein diacetate, succinimidyl ester

CPM, count per minute

CTL, cytotoxic T lymphocyte

ELISA, enzyme-linked immunosorbent assay

ELISPOT, enzyme-linked immunosorbent spot assay

FACS, fluorescence-activated cell sorter

FBS, fetal bovine serum

HLA-A2, human leukocyte antigen-A2

***i.p.*,** intra peritoneal

***i.v.*,** intra venous

IFN, interferon

IL, interleukin

MACS, magnetic-activated cell sorter

MDSC, myeloid derived suppressor cell

MHC, major histocompatibility complex

NK cells, natural killer cells

NKT cells, natural killer T cells

NOS2, nitric oxide synthase 2

Opn, osteopontin

PBS, phosphate buffered saline

SD, standard deviation

SEM, standard error means

VLA-4, very late antigen-4 (CD29/CD49d)

Part I.

Tumor-derived osteopontin act as an immune suppressor factor through accumulating myeloid-derived suppressor cells (MDSCs)

I. 1. Introduction

Tumors can escape host immune surveillance by recruiting various tumor associated myeloid cells (TAMCs) which represent immune-suppressive and protumoral characteristics [1]. Stemming from bone marrow common myeloid progenitors (CMP), they are consisted of heterogeneous myeloid cell populations such as tumor associated macrophages (TAM), tumor associated neutrophils (TAN), $Tie2^{+}$ monocyte (TEM) and myeloid derived suppressor cells (MDSCs) [2, 3]. Among them, MDSCs which are known as heterogeneous population of monocytic and granulocytic immature cells [4] are a key component for establishing tumor-derived immunosuppressive network [5]. The MDSCs are accumulated in diverse inflammatory conditions including tumor, and suppress multiple immune effectors mainly through reactive oxygen species (ROS) production, nitric oxide (NO) production, and arginase-1 secretion [6-12]. In the cancer patients, increment of peripheral MDSCs is clinically correlated with poor prognosis [9, 13-15]. Although several tumor-derived factors have known to relate with induction and accumulation of MDSCs, [14, 16-21]it is still elusive how MDSCs are generated and accumulated in the tumor environment.

In general, immune cells were originated from pluripotent $lineage^{neg}/CD127^{-}/CD117^{+}/Sca1^{+}$ hematopoietic stem cells (LSK cells). The LSK cells further differentiated into $lineage^{neg}/CD127^{-}/CD117^{+}/Sca1^{-}$ myeloid progenitor populations (LK cells) or $lineage^{neg}/CD127^{+}/CD117^{+}/Sca1^{+}$ common lymphoid progenitors that

could determine myeloid or lymphoid lineage of differentiating cells. In inflammatory conditions, the MDSCs are differentiated from myeloid progenitor cells, called myelopoiesis.

Chronic inflammatory environment such as in tumor could induce dysregulation of hematopoiesis, which cause excessive myelopoiesis in bone marrow and in turn increases MDSCs [7, 9, 22]. Additionally, tumor-induced myelopoiesis could occur in the outside of bone marrow particularly in spleens [1, 23-25], called extramedullary myelopoiesis which presumably provide another route for MDSC generation. Although it is assumed that inflammation mediators contribute to tumor-induced extramedullary myelopoiesis, responsible factors and its contribution remains unclear.

In this study, we screened responsible factors for extramedullary myelopoiesis in the tumor context using cytokine array. We found augmented osteopontin in both spleen lysates and sera in the tumor bearing mice and osteopontin was mainly produced by tumor cells. The osteopontin was originally known to bone matrix protein [26]. Recently, it has emerged as an inflammation mediator and has involved in tumor metastasis [27-29]. Based on this, we investigated whether tumor-derived osteopontin affect extramedullary myelopoiesis and MDSC accumulation in the tumor environment. Knock down osteopontin in the tumor cells and neutralizing of osteopontin showed reduced tumor growth, splenomegaly and extramedullary myelopoiesis in the tumor bearing mice. In the

primary cultured bone marrow cells and splenocytes, osteopontin increased the proliferation of LK cells. Moreover, osteopontin increased migration of bone marrow derived myeloid progenitor cells. Furthermore, osteopontin enhanced suppressive function of the MDSCs which differentiated from LK cells and subsequently inhibited T cell responses against tumor antigen. Therefore, these findings showed that tumor-derived osteopontin act as an immune suppressor factor through the generation of functional MDSCs.

I. 2. Materials and methods

Mice and tumor model

BALB/c mice and C57BL/6 were purchased from the Charles River Laboratories (Seoul, Korea). All mice maintained in specific pathogen-free (SPF) conditions in the Animal Center for Pharmaceutical Research at Seoul National University. The International Animal Care and Use Committee (IACUC) of Seoul National University approved the all animal experiments conducted in this study. For mice tumor model, the 3 x 10^5 cells of indicated tumor cells were injected subcutaneously into left flake of naïve mice.

Cell culture

MPIIB10 hybridoma was purchased from Developmental Studies Hybridoma Bank (Iowa City, IA, USA) and cultured in RPMI medium (GIBCO, Grand Island, NY, USA) that was supplemented with 10% FBS (GIBCO) and 1% penicillin/streptomycin (Lonza, Walkersvile, MD, USA) and 50μg/ml of Geneticin (GIBCO). CT26 colon calcinoma cells were cultured in DMEM medium that was supplemented with 10% FBS (GIBCO) and 1% penicillin/streptomycin (Lonza).

Mouse osteopontin lentiviral vector and shRNA transfection

The GIPZ lentiviral shRNA vector for mouse osteopontin knock-down (RMM4532-NM_009263, pGIPZ-shOpn) and GIPZ non-silencing lentiviral

shRNA control (RHS4346, pGIPZ) was purchased from Open Biosystems (Seoulin, Sung-Nam, Gyung-Gi, Korea). The Trans-lentiviral shRNA packaging kit was used for lentiviral particle production according to manufacturer's instructions (Open Biosystems). To establish osteopontin knock-downed CT26 cells or its control cells, the pGIPZ-shOpn or control pGIPZ containing lentiviral particles were transfected to CT26 cells respectively. The transfected CT26 cells were selected and subcloned in 10μg/ml puromycin containing DMEM medium supplemented with 10% FBS (GIBCO) and 1% penicillin/streptomycin (Lonza).

Ki-67 staining and cell number measurement

The $2x10^4$ of CT26shopn or CT26pGIPZ cells were cultured on 8-well chamber slide plates. After 2-day culture, cells were harvested and fixed by 70% ethanol and then, cells were stained with the alexa647-conjugated Ki67 antibody (M-19, Santacruz, Delaware, CA, USA). To count the cell number, the cells were fixed with 4% paraformaldehyde, and then stained with Hoechst 33342, nucleus marker (Invitrogen, KDR biotech, Seoul, Korea). The fluorescent images were acquired at 350nm excitation by the fluorescence microscope, and cell numbers were counted by the image J software (Free software distributed by NIH).

Flow cytometry analysis and ELISA

Almost all antibodies for flow cytometry were purchased from either Biolegend (San Diego, CA, USA) or BD Bioscience (San Jose, CA, USA). To detect

hematopoietic stem cells and myeloid progenitor cells, mice splenocytes were stained with FITC-conjugated lineage markers (CD3ε, B220, CD11b, Gr1, TER-119), FITC or APC-cy7-conjugated CD127 (A7R34), PE or APC-conjugated CD16/32 (93), PE-cy7-conjugated CD117 (2B8), PE-cy5-conjugated Sca-1 (D7) and APC or eFluor® 450-conjugated CD34 (RAM34). To analysis the surface molecules on myeloid progenitor cells, APC-conjugated CD29 (HMß1-1) and CD44 (IM7) and PE-conjugated CD49d (R1-2) were used. To detect MDSCs and T cells, mice splenocytes were stained with FITC-conjugated Ly6C (HK1.4), PE-cy7-conjugated Ly6G (1A8), APC-conjugated CD11b (M1/70), PerCP-cy5.5-conjugated CD4 (GK1.5), APC-cy7-conjugated CD8α (53-6.7), PE or eFluor® 450-conjugated CD3ε (145-2C11). For functional analysis of $CD3\varepsilon^+$ cells, mice splenocytes were intracellulary stained with PE-conjugated CD3ζ (H146-968, Santacruz). The flow cytometric analysis was performed using FACSAriaIII (BD Bioscience).

For osteopontin ELISA and western blot, goat-anti-mouse osteopontin was purchased from Sigma (Sigma Aldrich Korea, Seoul, Korea) and biotinylated goat-anti-mouse osteopontin was purchased from R&D systems (Minneapolis, MN, USA). Recombinant mouse (rm) osteopontin was purchased from R&D systems.

Cytokine array

For screening of the various cytokine levels in the mouse spleen lysate, Cytokine array kits (ARY-015 and ARY-006) were used according to manufacturer's

instruction. The mean spot density was measured by Image J software (Free software distributed by NIH), and mean values above reference (mean spot density of negative control spot) were charted on a graph using Graph Pad Prism software (La Jolla, CA, USA).

Quantitative real-time PCR

The RNaeasy Mini Kit (Quiagen, Valencia, CA, USA) were used for the preparation of total mRNA and amfiRivert Platinum (GenDEPOT, Baker, TX, USA) were used for cDNA synthesis. The synthesized cDNA and primers were mixed with SYBR Premix Ex Taq (Takara, Otsu, Shiga, Japan) and quantitative realtime PCR was performed on a LightCycer optical system (Roche, Basel, Switzerland). The following primers were used: murine *Hprt* forward (AAG ACT TGC TCG AGA TGT CAT GAA), and murine *Hprt* reverse (ATC CAG CAG GTC AGC AAA GAA), murine *Spp1* forward (CCG AGG TGA TAG CTT GGC TT), murine *Spp1* reverse (CTG CCC TTT CCG TTG TTG TC), murine *Nos2* forward (AGG AAG TGG GCC GAA GGA), murine *Nos2* reverse (GAA ACT ATG GAG CAC AGC CAC AT), murine *Arg1* forward (AAC ACG GCA GTG GCT TTA ACC), murine *Arg1* reverse (GTG ATG CCC CAG ATG GTT TTC), murine *Pu.1* forward (GCC TCA GTC ACC AGG TTT CC), murine *Pu.1* reverse (CTC TCA CCC TCC TCC TCA TCT G).

Bromodeoxyuridine (BrdU) incorporation

For *in vivo* BrdU incorporation analysis, the 500mg/Kg of Bromodeoxyuridine (BrdU) was injected intraperitonealy into CT26pGIPZ or CT26shOpn tumor bearing mice. Mice sacrificed at the 26-day after tumor injection, and the surfaces of splenocytes and bone marrow cells were stained for flow cytometric analysis. Then, incorporated BrdU were intracellulary stained using APC BrdU Flow Kit (BD Pharmigen^{TM}, San Jose, CA, USA). For *in vitro* BrdU incorporation analysis, total splenocyte and bone marrow cells from CT26 tumor bearing mice (2 week) were cultured in STEMPRO34 serum free medium (GIBCO) supplemented with 1% penicillin/streptomycin (Lonza), 2mM L-glutamic acid (Lonza), nutrient supplement (GIBCO, 40X stock supplemented with STEMPRO34), 10ng/ml rmIL3 (eBioscience), 20ng/ml rmIL6 (eBioscience), 10ng/ml rmSCF (R&D) (STEMPRO34 complete medium) with or without 2μg/ml osteopontin. After 24-hr culture, BrdU was added to make 1 μg/ml of final concentration and incubated for an additional 24 hrs. Incorporated BrdU were measured as described above.

***In vivo* CTL and *in vitro* IFNγ production**

The *in vivo* CTL assay was performed as previously described [30]. Briefly, equal amount ($5x10^6$) of 20μM CFSE-labeled, 2 μg/ml AH1 peptide loaded naïve balb/c splenocytes and 2.5 μM CFSE labeled naïve balb/c splenocytes were mixed and intravenously injected into the CT26shOpn or CT26pGIPZ tumor bearing mice.

The AH1 peptide, H-2^d epitope peptide of gp70 of CT26 tumor (AH1 6-14, SPSYVYHQF) was purchased from AnyGen (Jang-Seoung, Jeonnam, Korea). After 18-hr target cell injection, mice were sacrificed and AH1-specific target lysis was analyzed by flow cytometry. The specific lysis was calculated as follows: r (ratio)=(% $CFSE^{low}$/% $CFSE^{high}$), % lysis=[1–($r^{unprimed}$/r^{primed})]x100

For *in vitro* IFNγ production, the $1x10^8$ cells of total splenocyte of the CT26shOpn or CT26pGIPZ tumor bearing mice were re-stimulated with the 5 μg/ml AH1 peptide or 50 μg/ml mitomycin C-treated CT26 ($5x10^6$ cells) for five-day. The *in vitro* culture medium was RPMI medium supplemented with 1% penicillin/streptomycin, 10% FBS, 10mM HEPES, 1mM sodium pyruvate, 0.1mM nonessential amino acid (NEAA) and 0.05mM ß-mercaptoethanol. The IFNγ levels on the culture supernatant were determined by mouse IFNγ ELISA kit (BD bioscience, San Jose, CA, USA) according to manufacturer's instruction.

Osteopontin neutralizing experiment

The mice were subcutaneously injected CT26pGIPZ or CT26shOpn tumors ($3x10^5$ cells). The 7 days after tumor injection, 300 μg MPIIIB10 or control mouse IgG (Sigma) were intraperitoneally injected to these mice every three days. The 21 days after tumor injection, mice were sacrificed and various immune cells in the spleen were analyzed by flow cytometry.

Transwell

The total bone marrow cells were isolated from 2 week CT26 tumor bearing mice. Myeloid progenitor cells were enriched by depletion of the Ly6G, Ly6C, CD3, B220 positive cells using microbead and MACS (Miltenyi Biotec, Bergisch Gladbach, Germany). Then, the $Lin^-/CD127^-/CD117^+/Sca1^-$ myeloid progenitor cells were sorted using FACSAriaIII (BD Bioscience) and $1x10^5$ sorted cells were suspended in the 100µl STEMPRO34 medium and plated upper well of 24-transwell plate (8µm pore size, Corning Cosatar, Tewksbury MA 01876, USA). In the lower well, 2µg/ml osteopontin or vehicle (PBS) were added in STEMPRO34 complete medium and incubated for 18hrs. Then, cells in the lower well were harvested, fixed on the slide glass and Hematoxylin & eosin stained by DiffQuick Staining Kit (Sysmex, Chuo-ku, Kobe, Japan). Migration index was measured by counting the cells in the lower well using ImegeJ software.

Statistics

The data were shown as the means ± SEM. Statistical significance was analyzed by Graph Pad Prism software (La Jolla, CA, USA). A two-tailed Student's *t*-test or two-way ANOVA were used to calculate statistical significance and p values <0.05 were considered significant at a 95% confidence interval.

I. 3. Results

Extramedullary myelopoiesis was increased in tumor bearing mice

It is well known phenomenon that MDSCs rapidly accumulated in spleen and tumor site as tumors grew. At 21 days after tumor injection, the number of total splenocyte was increased two fold in the CT26 tumor bearing mice (Figure 1A). The percentages and number of both Mo MDSCs ($CD11b^{+}/Ly6C^{hi}/Ly6G^{lo}$) and PMN MDSCs ($CD11b^{+}/Ly6C^{lo}/Ly6G^{hi}$) were greatly increased in the spleens of tumor bearing mice (Figure 1B and 1C). In the contrast, percentages of $CD4^{+}$ and $CD8^{+}$ T lymphocytes were decreased (Figure 1D). Due to splenomegaly of tumor bearing mice, numbers of T lymphocytes were not changed (Figure 1E).

Inflammatory stimuli such as tumor could induce hematopoietic proliferation and differentiation in the spleen as well as in bone marrow [1, 23-25]. Next we analyzed hematopoietic stem cell populations ($Lineage^{neg}/CD127^{-}/CD117^{+}/Sca1^{+}$, LSK cells) and heterogeneous myeloid progenitors ($Lineage^{neg}/CD127^{-}/CD117^{+}/Sca1^{-}$, LK cells) in the spleen of CT26 tumor bearing mice (Figure 2A). Comparing to splenocyte of naïve mice, we observed greatly increased LK cells and LSK cell in the splenocyte of tumor bearing mice (Figure 2B and 2C) which indicated that splenic myelopoiesis was increased in the tumor context, consequently responsible for MDSC expansion.

Osteopontin increased in the tumor environment

To find responsible factors for tumor-induced extramedullary myelopoiesis in spleen, we screened levels of various cytokines in the spleen lysate of naïve and tumor bearing mice by cytokine array. As a result, CD26, CXCL1, CCL2 and osteopontin were increased in the spleen of tumor bearing mice comparing to cytokine levels in the naïve mice spleen (Figure 3A and 3B). However, because the role of osteopontin on extramedullary myelopoiesis has been unknown, we sought to determine whether osteopontin is responsible for splenic extramedullary myelopoiesis in the tumor context. To confirm cytokine array data, we analyzed amount of osteopontin in the spleen lysate and sera of tumor bearing mice by ELISA. The osteopontin was significantly increased in the both spleen lysate and sera of CT26 tumor bearing mice (Figure 3C). Using real time PCR analysis, we found that increased osteopontin was mainly produced by tumor tissue (Figure 3D).

In addition, we observed similar results in other tumor model, MC38 tumor bearing mice, which showed splenomegaly (Figure 4A), accumulated MDSCs in spleen (Figure 4B) and increased splenic LSK and LK cells (Figure 4C) in the tumor context. The level of osteopontin also increased in the spleen lysate and sera of MC38 tumor bearing mice (Figure 4D) and tumor cells dominantly produced osteopontin (Figure 4E).

Extramedullary myelopoiesis was induced by tumor-derived osteopontin

To determine whether tumor-derived osteopontin affect splenic extramedullary myelopoiesis in the tumor context, we established osteopontin knock-downed CT26 tumor cell line using transfection osteopontin shRNA containing lentiviral vector (CT26shOpn). The CT26 cells transfected with control lentiviral vector were used as control cell line (CT26pGIPZ). We observed osteopontin was successfully knock-downed in the CT26shOpn (Figure 5A) and lentiviral vector transfection did not affect *in vitro* proliferation of CT26shOpn and CT26pGIPZ cells (Figure 5B).

Next, we subcutaneously inoculated these CT26pGIPZ and CT26shOpn tumor cells to naïve balb/c mice. Compared to CT26pGIPZ group, the CT26shOpn group showed retarded tumor growth (Figure 5C) which suggests that tumor-derived osteopontin may be involved in *in vivo* growth of tumors. The 21 days after tumor inoculation, mice were sacrificed and various immune cells and progenitor cells in the spleen were analyzed by flow cytometry. In the CT26shOpn group, total splenocytes were lesser and osteopontin levels in the serum and tumor tissue were lower than those of CT26pGIPZ group (Figure 5D). The CT26pGIPZ group and CT26shOpn group showed higher percentages and numbers of the LK cells and LSK cells in the spleen than those of naïve group. However, the increase rate of splenic LK cells in the CT26shOpn group was lower than the CT26pGIPZ group while increase rate of splenic LSK cell in these groups looked same (Figure 5E and

5F). These data indicate that tumor-derived osteopontin might be related to splenic LK cell increase and subsequently increase extramedullary myelopoiesis in the tumor environment.

The percentages and numbers of Mo MDSC and PMN MDSC were greatly increased in the spleen of CT26pGIPZ group along with the LK cell increase in this group (Figure 6A). The CT26shOpn group also showed higher percentages and numbers of Mo MDSC, PMN MDSC than naïve group however, increase rate of these cells were lower than CT26pGIPZ group (Figure 6A). In addition, the numbers of tumor infiltrated Mo MDSC and PMN MDSCs in the CT26pGIPZ group were higher than CT26shOpn group (Figure 6D).

The changes of macrophage ($CD11b^+/F4/80^+$) and myeloid dendritic cells ($CD11b^+/CD11c^+$) in the CT26pGIPZ group and CT26shOpn group showed a similar tendency with the changes of MDSCs in these groups. Although macrophage and myeloid dendritic cells were greatly increased in the CT26pGIPZ group, expression of MHC class II molecule on these cells were lower than that of naïve group implying antigen presenting functional defect of these cells (Figure 6D).

Due to splenomegaly in the CT26pGIPZ group, percentage of $CD4^+$ T cells and $CD8^+$ T cells was reduced while number of these cells did not changed (Figure 6B). The changes of $CD4^+$ T cells and $CD8^+$ T cells in the CT26shOpn group were

similar to CT26pGIPZ group except slightly increased number of $CD8^+$ T cells (Figure 6B).

Neutralizing of osteopontin ameliorated splenomegaly and proliferation of myeloid progenitor cells.

Next, we neutralized osteopontin in the tumor bearing mice to test whether extramedullary myelopoiesis was inhibited by systemic neutralization of osteopontin in tumor environment. We inoculated MC38 tumor cells to C57BL/6 mice .Seven days after tumor inoculation, we intraperitoneally injected 300ug of MPIIIB10 (anti-Opn mIgG) or control mIgG every three days. We observed tumor growth inhibition in the anti-Opn mIgG treated mice (Figure 7A). These anti-Opn mIgG treated mice showed reduced splenomegaly and lower osteopontin level in the serum than those of control mIgG treated mice (Figure 7B and 7C). The percentage and number of splenic LK cells was also reduced in the anti-Opn mIgG treated mice (Figure 7D). Although osteopontin neutralization didn't reduce the percentages of Mo MDSC and PMN MDSC in the spleen, the number of Mo MDSC and PMN MDSC was decreased due to reduced splenomegaly (Figure 7E and 7F). These results implicated that osteopontin affect LK cell accumulation in the spleen of tumor bearing mice and subsequently induce extramedullary myelopoiesis which could lead accumulation of MDSCs.

Tumor-derived osteopontin increased proliferation of myeloid progenitor (LK) cells

To investigate an effect of osteopontin in tumor-derived extramedullary myelopoiesis in spleen, we tested LK cell proliferation in the CT26pGIPZ or CT26shOpn tumor bearing mice by measuring an incorporated bromodeoxyuridine (BrdU) in LK cells. As shown in Figure 5C, tumor growth was inhibited in the CT26shOpn inoculated mice (Figure 8A). The incorporated BrdU in the LK cells from spleen and bone marrow were measured by flow cytometry. The BrdU incorporation of bone marrow LK cells was not distinguishable in the naïve, CT26pGIPZ and CT26shOpn group. However, the BrdU incorporation was increased in the splenic LK cells of CT26pGIPZ group (Figure 8B). In the *in vitro* culture of total splenocytes and bone marrow cells, osteopontin enhanced proliferation of both spleen and bone marrow LK cells (Figure 8C).

Next, we analyzed various osteopontin receptors on LK cells from spleen or bone marrow. There was no significant difference in CD29 (integrin ß1) expression between spleen LK cells and bone marrow LK cells. However, expressions of CD49d (integrin α4) and CD44 were higher in the splenic LK cells than those of LK cells in bone marrow. Moreover, the expressions of these molecules were up-regulated in the tumor environment (Figure 8D). These results suggest that osteopontin might induce proliferation of splenic LK cells through VLA4 (integrin α4/ ß1) or CD44 mediated pathway in the tumor bearing host.

Osteopontin increased migration of LK cells in bone marrow

Next, we questioned whether osteopontin could induce migration of bone marrow LK cells. To test this, we plated bone marrow LK cells on the upper well of transwell and measured cell migration toward lower well (Figure 9A). The more bone marrow LK cells migrated to lower well when osteopontin exist in the lower well (Figure 9B). These data suggest that tumor-derived osteopontin increased migration of bone marrow LK cells and subsequently contribute to splenic extramedullary myelopoiesis.

Osteopontin aggravated tumor-derived immunosuppressive environment

As shown in previous figures, tumor derived osteopontin increased proliferation of splenic LK (myeloid progenitor) cells (Figure 8) and migration of bone marrow LK cells (Figure 9) which contributed to extramedullary myelopoiesis in spleen in the tumor environment. Next, we questioned whether osteopontin affect the suppressive function of MDSCs. We differentiated LK cells to myeloid cells using GM-CSF with or without osteopontin for 7 days. We observed that over the 90% of differentiated cells expressed $CD11b^{+}/Gr1^{+}$ which represent a typical phenotype of MDSCs (Figure 10A). In addition, we analyzed mRNA expressions related with

suppressive function and maturity of MDSCs. The differentiated myeloid cells of GM-CSF&Opn group expressed less *Pu.1* mRNA and higher *Nos2* mRNA than those of differentiated cells of GM-CSF group indicating more immature and suppressive characteristics of these cells (Figure 10B). To measure suppressive activities of differentiated cells, these cells were co-cultured with OT1 splenocytes and OVA-specific proliferation of OT1 cells were measured by ^{3}H thymidine uptake. The GM-CSF&Opn group more effectively inhibited OVA-specific proliferation of OT1 splenocytes than that of GM-CSF control group (Figure 10C). Similar result was obtained in the co-culture of OT1 cells and MDSCs derived from CT26pGIPZ tumor bearing mice (Figure 10D). However, osteopontin did not affect suppressive function of already differentiated MDSCs (Figure 10E). These data indicated that, osteopontin affected differentiation process of LK cells and subsequently generated more suppressive MDSCs from these cells.

Nest, we investigated whether tumor-derived osteopontin could cause functional defect in T cell responses through MDSCs. We observed CD3ζ down-regulation in the $CD3^{+}$ splenocyte of CT26pGIPZ bearing mice indicating functional defect of activation signaling transduction of T cells. In the $CD3^{+}$ splenocyte of CT26shOpn bearing mice, CD3ζ down-regulation was partially restored (Figure 10F). After *in vitro* re-stimulation of AH1 peptide or mitomycin C-treated CT26, the splenocyte of CT26pGIPZ group did not enhance the interferon-gamma (IFNγ) production compared with naïve group, whereas that of CT26shOpn group significantly

enhanced a level of IFNγ production (Figure 10G). The *in vivo* AH1-specific lysis were also reduced in the CT26pGIPZ group (Figure 10H). These results suggested that osteopontin aggravates tumor-derived immunosuppressive environment through generating more immunosuppressive MDSCs from myeloid progenitor cells and subsequently inhibits tumor antigen specific T cell responses.

I. 4. Discussion

Tumors can establish immune suppressive environment for their survival and progression [31]. For this, tumors secrete various soluble factors and recruit diverse immune suppressive myeloid cells [2, 3, 32]. Among them, MDSCs are considered as a key component for establishing tumor-derived immunosuppressive network [5]. Although there have been various studies targeting MDSCs to overcoming the tumor-derived immune suppressive environment [15, 30, 33], these approaches could not completely prevent generation of MDSCs. Therefore, there has been a demand for a new approach regarding to target MDSC generation. With the therapeutic targeting of MDSCs, blocking of the abnormal myelopoiesis would fundamentally eliminate tumor-derived immunosuppressive network. In this regard, we focused on the tumor-derive myelopoiesis and responsible factors for this.

In this study, we uncovered novel roles of tumor-derived osteopontin in extramedullary myelopoiesis. We found that osteopontin was significantly increased in CT26 and MC38 mouse tumor models. Knocking-down or neutralizing of tumor-derived osteopontin inhibited tumor growth and reduced extramedullary myelopoiesis. Consequently, these result alleviated MDSC accumulation in the spleen and tumor. Osteopontin increased the proliferation of LK cells and migration of bone marrow LK cells. Furthermore, osteopontin affect differentiation process of LK cells and differentiate them into more immunosuppressive MDSCs.

Accumulation of MDSCs in spleen and tumor site is commonly observed in tumor bearing host [7, 9, 30, 33]. We confirmed splenomegaly and MDSCs accumulation in the early stage of (3 week) tumor bearing mice (Figure 1A-C, 4A and 4B). Although MDSCs were increased in these mice, number of $CD8^+$ T cell and $CD4^+$ T cell did not changed (Figure 1D and 1E). These results indicated that abnormally accumulated MDSCs are a main factor of enlarged spleens in tumor context.

In general, expansion of myeloid cells occurs in the chronic inflammatory conditions including in tumor, which is accompanied with excessive myelopoiesis [7, 9, 22]. Although bone marrow has been generally considered as a site of myelopoiesis, myelopoiesis could occur in the outside of bone marrow particularly in spleen in various inflammatory conditions [1, 23-25]. Recent studies have been suggested that spleen emerged as a myeloid reservoir and responsible for generating immunosuppressive myeloid cells in inflammatory conditions [1, 34, 35]. In consistence with this, we observed that hematopoietic stem cell populations (Lin^{neg}/ $CD127^-/CD117^+/Sca1^+$, LSK cells) and heterogeneous myeloid progenitor populations ($Lin^{neg}/CD127^-/CD117^+/Sca1^-$, LK cells) were increased in the spleen of tumor bearing mice (Figure 2 and 4C). These results indicated that splenic extramedullary myelopoiesis was increased in tumor environment.

Although various tumor derived factors and inflammatory mediators should be involved in extramedullary myelopoiesis, which specific factors are critical is still elusive. Therefore, we investigated responsible factors for extramedullary

myelopoiesis in the tumor bearing mice. As a result, we found that osteopontin was augmented in the CT26 and MC38 tumor bearing mice, which were mainly derived from tumors (Figure 3, 4D and 4E). Since tumors express 160 fold-high osteopontin mRNA than that of Mo-MDSC, entire increase of osteopontin in tumor bearing mice might be derived from tumor cells rather than Mo MDSCs (Figure 3D). Therefore, we intensively studied roles of osteopontin in extramedullary myelopoiesis.

Osteopontin is a member of small integrin-binding ligand N-linked glycoproteins (SIBLINGs) family which is abundantly found in extracellular matrix and body fluids [26, 36, 37]. It was primary known to bone sialoprotein which mediate bone resorption through binding of osteoclast to the mineralized bone matrix [38]. In immune system, it has been known to be an early T cell activator (ETA-1) cytokine that promotes Th1 inflammatory responses through inhibition of Th2 cytokine production and is associated with several autoimmune disease [39, 40]. Recently, osteopontin has been revealed as an inflammatory mediator and several reports have showed overexpression of osteopontin on various tumors, and have suggested osteopontin as a prognosis marker for the prediction of tumor malignancy [41-44]. In several tumors, osteopontin has been known to enhance their growth and metastasis [45]. Osteopontin induce proliferation of preneoplastic fibroblast cells through CD44 mediated MAPK pathway [46] and inhibition of osteopontin expression by siRNA reduced *in vitro* growth of melanoma cells [47]. Osteopontin

down-regulation decreased proliferation and metastasis through MEK/Erk1/2 pathway in the human hepatocellular carcinoma xenograft tumor model [48]. In addition, osteopontin enhanced proliferation and migration of human breast cancer cells through integrin αv/ß3 mediated JAK/STAT3 signaling [29]. However, it was reported that knock-down of osteopontin through siRNA reduced the invasion and metastasis without affect *in vitro* cell proliferation in CT26 colon adenocarcinoma cells [49]. In consist with this, we observed that lentiviral knock-down of osteopontin did not affect the *in vitro* proliferation of CT26 cells (Figure 5B). Since osteopontin is not sole factor for the proliferation of tumor cells, other growth factors may crucial for the proliferation of CT26 cells rather than osteopontin. Different to *in vitro* proliferation of CT26shOpn, *in vivo* tumor growth of CT26shOpn was significantly inhibited (Figure 5C). This result suggests that osteopontin is crucial for establishing tumorigenic environment which could support the growth of tumor in *in vivo*.

Besides the inhibition of tumor growth, CT26shOpn bearing mice showed the reduced splenomegaly and extramedullary myelopoiesis, which subsequently reduced MDSC accumulation in both spleen and tumor site (Figure 5 and 6). In spleen, osteopontin knock-down in tumor did not prevent to accumulate the precursor of LK cells (LSK cells) (Figure 5G), whereas LK cells decreased in the osteopontin knock-downed tumor bearing mice. This result was further supported by osteopontin neutralizing in the MC38 moues tumor model (Figure 7). Taken

together, these results suggest that tumor-derived osteopontin could affect expansion of LK cells and subsequently increases MDSCs in the tumor context.

Moreover, we observed that osteopontin increased proliferation of LK cells in the spleen, not in the bone marrow in the mouse tumor model (Figure 8B). The different reactivity on osteopontin in spleen and bone marrow LK cells is presumably due to the different expression patterns of CD44 or CD49d on the LK cells in spleen and bone marrow (Figure 8D). However, osteopontin increased the proliferation in both splenic and bone marrow LK cells under *in vitro* culture condition (Figure 8C) in spite of different expression pattern of CD44 and CD49d. This discrepancy may due to different environment between *in vivo* and *in vitro* conditions. It is possible that tumor-derived osteopontin poorly distributed to bone marrow and insufficient osteopontin did not increase the proliferation of LK cells. Additionally, various factors in the bone marrow might prevent the proliferation of bone marrow LK cells in the CT26pGIPZ tumor model. In our *in vitro* culture condition, it seems that exogenously added osteopontin might be sufficient to induce proliferation of LK cells regardless of expression intensity of CD44 and CD49d.

The role of osteopontin in the proliferation of stem cells or progenitor cells is still controversial. For instance, several reports have been showed that osteopontin is a key component of hematopoietic stem cell niche and negatively regulate hematopoietic stem cells in the bone marrow [50, 51]. However, in the presence of

fibroblast growth factor 2, osteopontin could promote proliferation of neural progenitor cells by PI3K-Akt intracellular signal transduction [52]. Since physiological environment is quite different between normal host and tumor bearing host, the role of osteopontin might depend on the surrounding environment of LK cells. Osteopontin-triggered signal transduction via integrins mainly relates with evasion and migration of tumor cells, whereas CD44 signal transduction involves in the cell survival and proliferation via PI3K-Akt and MAPK pathway [45, 46]. Thus, we assumed that CD44 is associated to the proliferation of splenic LK cell, despite precise intracellular mechanism should be investigated in further studies.

Tumor-derived osteopontin aggravated tumor immunosuppressive environment through the generation of suppressive MDSCs, and consequently caused functional defect in T cell responses (Figure 10). More suppressive MDSCs were differentiated from LK cells when osteopontin existed in the culture medium which indicated that osteopontin affected differentiation process of LK cells. Although osteopontin has been known to negatively regulate NOS2 expression [53], we observed that differentiated myeloid cells expressed higher NOS2 mRNA level in the GM-CSF&Opn group than that of GM-CSF group (Figure 10B). Since expression level of *Pu.1* mRNA was decreased in GM-CSF&opn group, we assume that osteopontin affected the differentiation of LK cells, which in turn increased the immaturity of differentiated myeloid cells and subsequently increased

NOS2 expression. It was reported that osteopontin down regulated Notch1 expression on human CD34+ hematopoietic cells [54]. In addition, down regulated Notch signaling in bone marrow myeloid progenitor cells have induced accumulation of MDSCs [55]. Taken together, decreased *PU.1* expression on differentiated cells of GM-CSF&Opn group might be involved in down-regulated Notch signaling, however underlying mechanisms should be investigated in the further studies.

In this study, we investigated the novel function of osteopontin in the extramedullary myelopoiesis in tumor. We demonstrated that tumor-derived osteopontin functions as an immune suppressor factor, which could aggravate immunosuppressive environment through excess extramedullary myelopoiesis. Furthermore, these findings suggest that osteopontin could become a novel therapeutic target to treat tumor-derived abnormal myelopoiesis and to overcome tumor immunosuppressive environment.

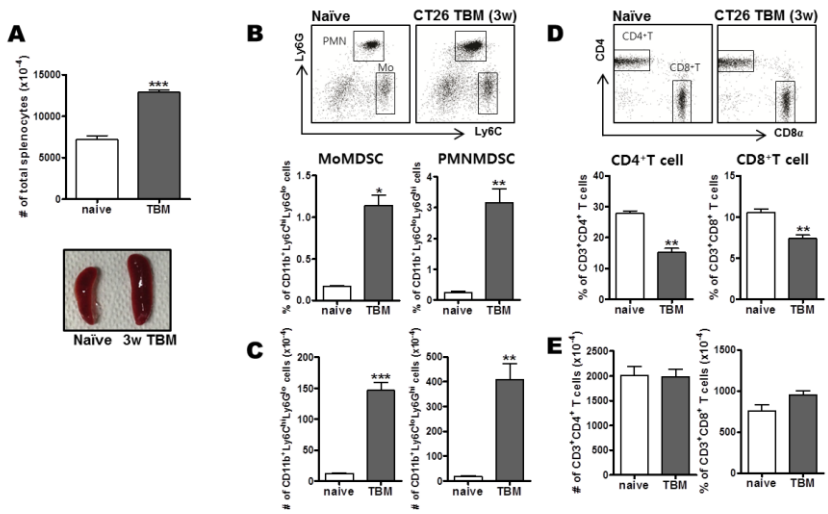

Figure 1. Increased splenic myeloid-derived suppressor cells and splenomegaly in tumor environment Balb/c mice were subcutaneously injected with $3x10^5$ of CT26 cells. (A) The 3 weeks after tumor injection, the number of total splenocyte were measured. (B and C) The numbers and percentages of monocytic (Mo) and granulocytic (PMN) myeloid-derived suppressor cells (MDSC) in the splenocytes of naïve or CT26 tumor bearing mice were analyzed by flow cytometry. (D and E) The numbers and percentages of $CD4^+$ T cells and $CD8^+$ T cells in the splenocytes of naïve or CT26 tumor bearing mice were analyzed by flow cytometry. All data are representative of three independent experiments (n=3, *P < 0.05, **P < 0.01, ***P < 0.001).

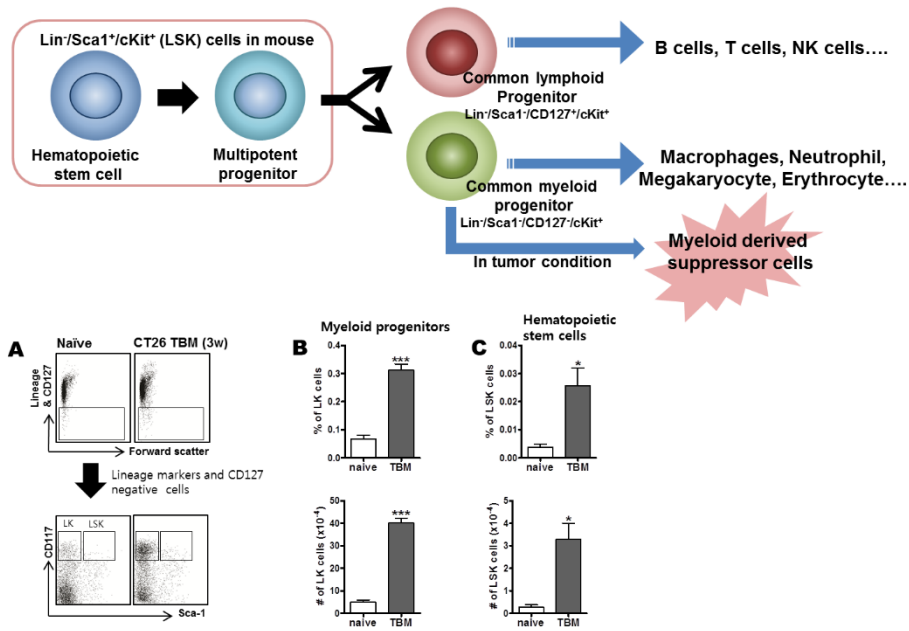

Figure 2 Enhanced extramedullary myelopoiesis in tumor environment (A) The $CD117^{+}/Sca1^{-}$ heterogeneous myeloid progenitor populations (LK cell) and $CD117^{+}/Sca1^{+}$ hematopoietic stem cell populations (LSK cells) were analyzed in the $Lin^{neg}/CD127^{-}$ splenocytes by flow cytometry. (B and C) The numbers and percentages of LK and LSK cells were charted on the graph. All data are representative of three independent experiments (n=3, *P < 0.05, **P < 0.01, ***P < 0.001).

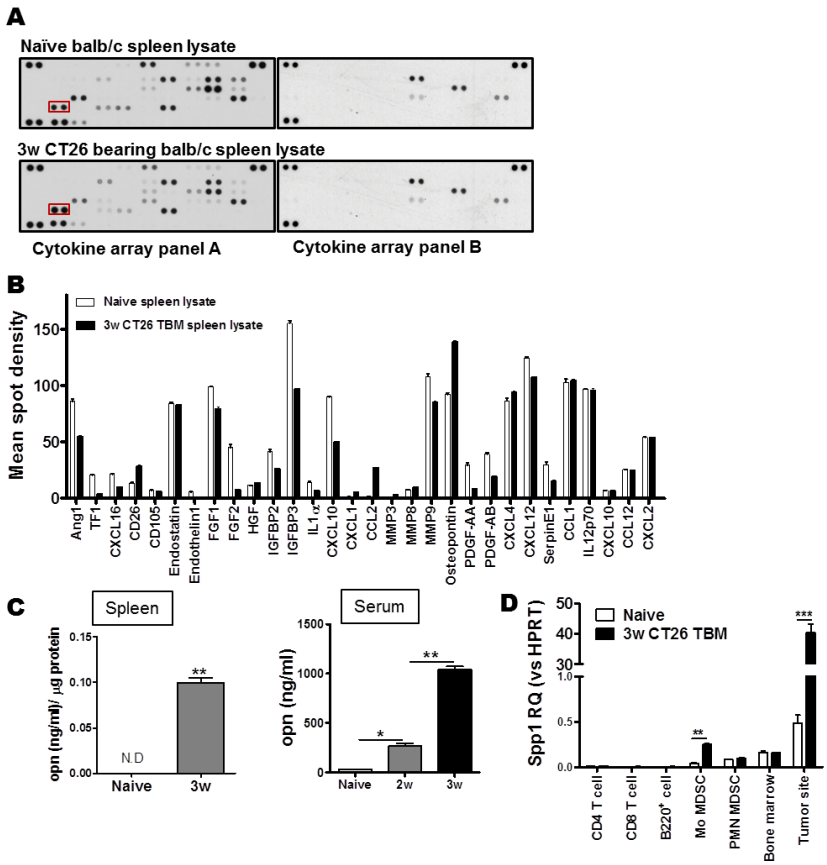

Figure 3. Osteopontin increased in the tumor environment (A) Cytokine levels in the spleen lysates of naïve balb/c mouse and CT26 tumor bearing mouse were blotted by cytokine array. (B) The mean spot densities of each spot were measured and then mean values above reference were charted on the graph. (C) The concentrations of osteopontin in serum and spleen lysate were measured by ELISA. (D) The *spp1* (osteopontin) mRNA levels were analyzed by quantitative real time PCR. All data are representative of two independent experiments (*P < 0.05, **P < 0.01, ***P < 0.001).

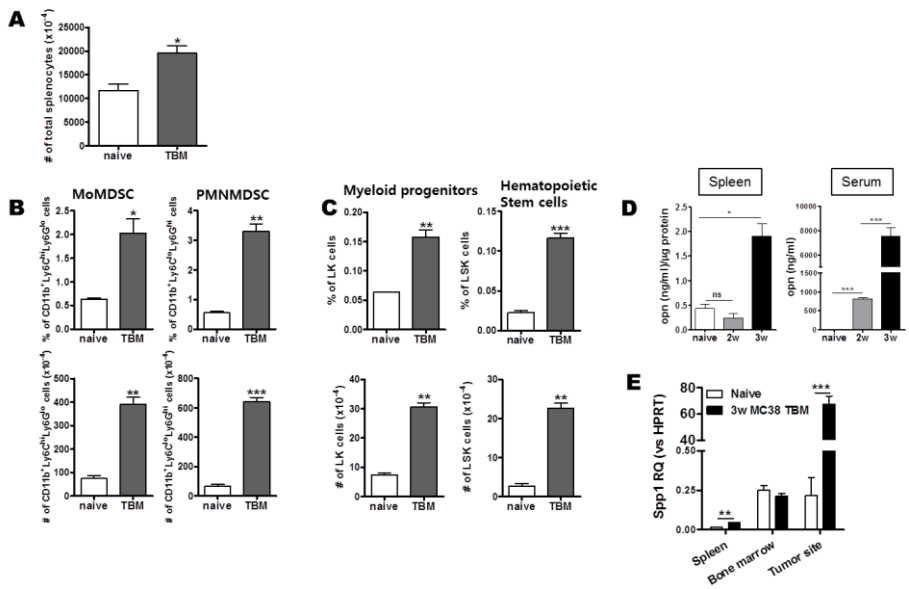

Figure 4. Enhanced extramedullary myelopoiesis and increased osteopontin in MC38 tumor bearing mice C57BL/6 mice were subcutaneously injected with $3x10^5$ of MC38 cells. (A) The 3 weeks after tumor injection, the number of total splenocyte were measured. The numbers and percentages of (B) Mo-MDSC, PMN-MDSC (C) LK cells and LSK cells in the splenocytes of naïve or MC38 tumor bearing mice were analyzed by flow cytometry (n=3). (D) The concentrations of osteopontin in serum and spleen lysates of naïve or MC38 tumor bearing mice were measured by ELISA. (E) The *spp1* mRNA levels were analyzed by quantitative real time PCR. All data are representative of two independent experiments (*P < 0.05, **P < 0.01, ***P < 0.001).

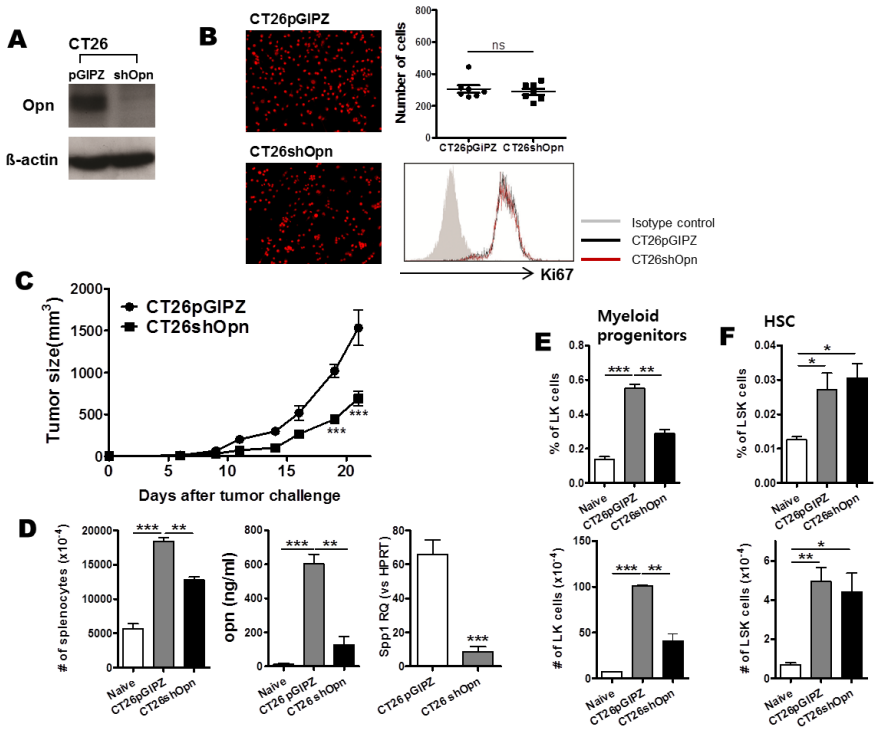

Figure 5. Splenic extramedullary myelopoiesis induced by tumor-derived osteopontin (A) Expression level of osteopontin protein in the CT26pGIPZ and CT26shopn cells were analyzed by western blot. (B) The $2x10^4$ cells of CT26pGIPZ and CT26shOpn were plated to 8-chamber plate. After two days, numbers of cells were counted by Hoechst staining and proliferating cells were analyzed by Ki67 staining. (C) Balb/c mice were subcutaneously injected with $3x10^5$ CT26pGIPZ or CT26shOpn cells. From seven days after tumor injection, tumor size was measured every two or three days (n=5). (D) Three weeks after tumor injection, mice were sacrificed and numbers of total splenocytes were measured. Additionally, osteopontin concentrations in the serum were determined

by ELISA and mRNA expressions of *spp1* in the tumor tissues were analyzed by quantitative real time PCR. (E and F) The percentages and numbers of LK cells and LSK cells in the splenocytes of naïve, CT26pGIPZ and CT26shOpn tumor bearing mice were analyzed by flow cytometry (n=3). All data are representative of two independent experiments (*P < 0.05, **P < 0.01, ***P < 0.001).

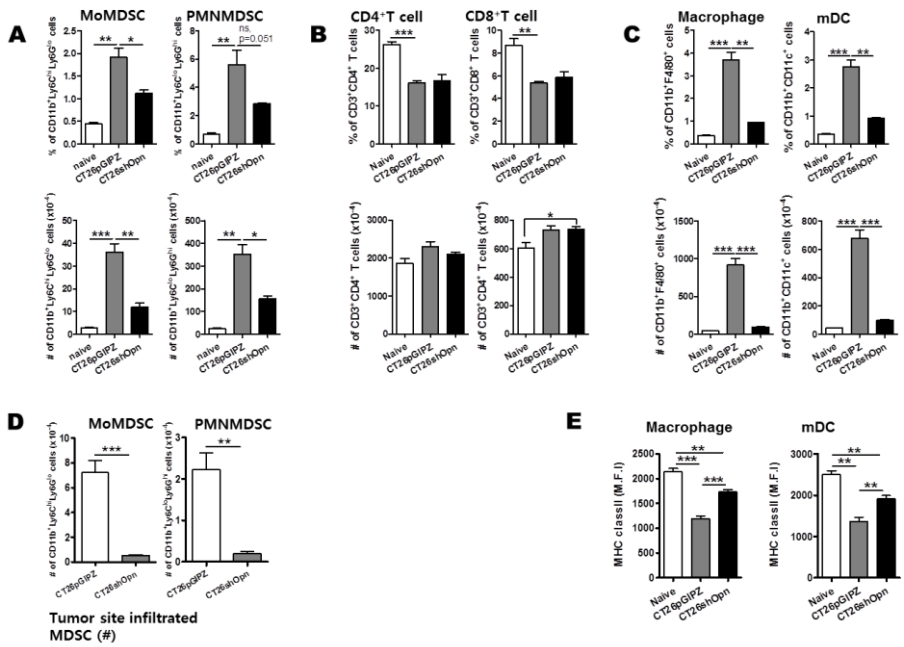

Figure. 6 Accumulation of peripheral myeloid cells by osteopontin-induced extramedullary myelopoiesis The percentages and numbers of (A) Mo-MDSC cells, PMN-MDSC cells, (B) $CD4^+$ T cells, $CD8^+$ T cells, (C) $CD11b^+/F4/80^+$ macrophages and $CD11b^+/CD11c^+$ mDCs in the splenocytes of naïve, CT26pGIPZ and CT26shOpn tumor bearing mice were analyzed by flow cytometry. (D) The total numbers of tumor infiltrated Mo-MDSC and PMN MDSC in the CT26pGIPZ or CT26shOpn tumor bearing mice were analyzed by flow cytometry. (E) The expression levels of MHC ClassII molecules on the $CD11b^+/F4/80^+$ macrophages and $CD11b^+/CD11c^+$ mDCs in the splenocytes of naïve, CT26pGIPZ and CT26shOpn tumor bearing mice. All data are representative of two independent experiments (n=3, *P < 0.05, **P < 0.01, ***P < 0.001).

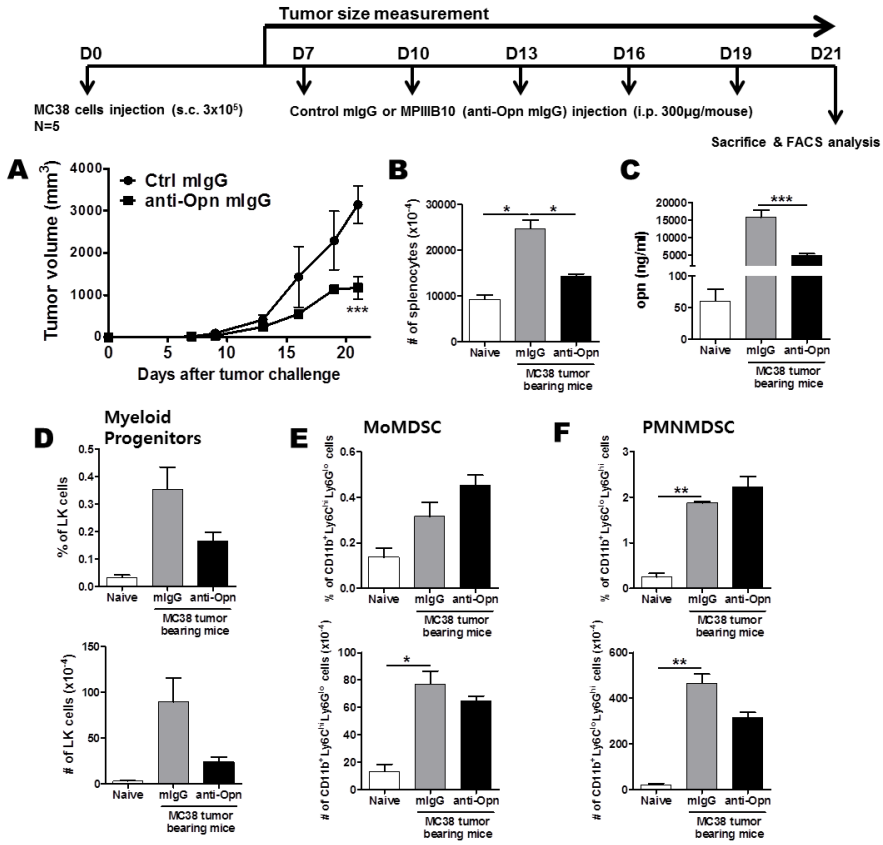

Figure 7. Neutralizing of osteopontin inhibited tumor growth, and ameliorated splenomegaly and accumulation of splenic myeloid progenitor cells (A) C57BL/6 mice were subcutaneously injected with $3x10^5$ of MC38 cells. From the seven days after tumor injection, 300μg of control mIgG or MPIIIB10 (anti-Opn mIgG) were intraperitonealy injected to mice and tumor size was measured (n=5). (B) Three weeks after tumor injection, mice were sacrificed and number of total splenocyte was counted. (C) Osteopontin concentration in the mice serum was determined by ELISA. The percentages and numbers of (D) LK cells, (E) Mo MDSC and (F) PMN MDSC in the splenocyte were analyzed by flow cytometry(n=3, *P < 0.05, **P < 0.01, ***P < 0.001).

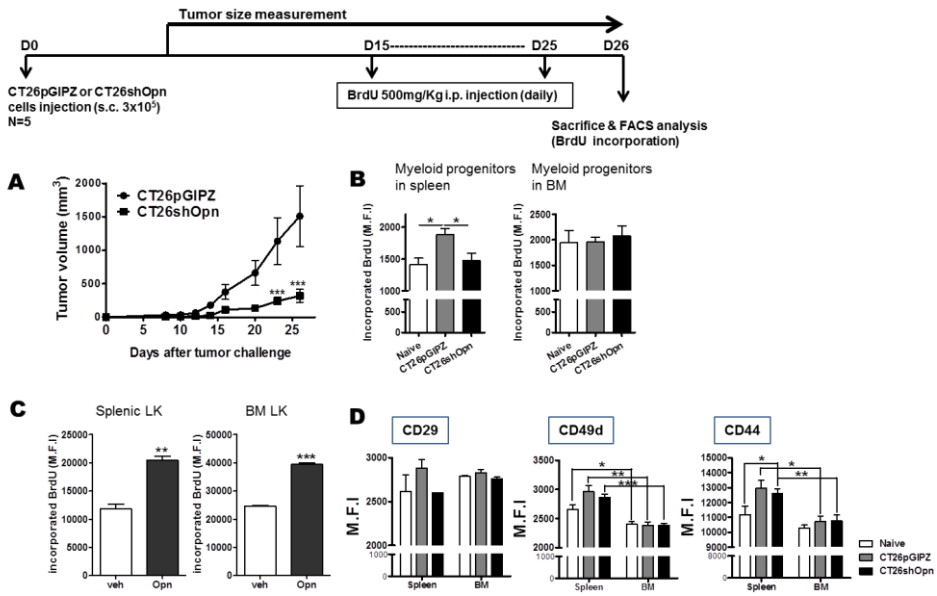

Figure 8. Tumor-derived osteopontin increased proliferation of myeloid progenitor cells

(A) Balb/c mice were subcutaneously injected with $3x10^5$ CT26pGIPZ or CT26shOpn cells and 500mg/Kg BrdU was daily injected from 15-25 days. From seven days after tumor injection, tumor size was measured every two or three days (n=5). (B) Incorporated BrdU in the spleen and bone marrow LK cells were analyzed by flow cytometry. (C) BrdU incorporation in LK cells of *in vitro* cultured total splenocyte and bone marrow cells from 2 week CT26 tumor bearing mouse. (D) The expression levels of CD29, CD49d and CD44 on the LK cells of naïve, CT26pGIPZ and CT26shOpn tumor bearing mice (n=3). All data are representative of two independent experiments (*P < 0.05, **P < 0.01, ***P < 0.001).

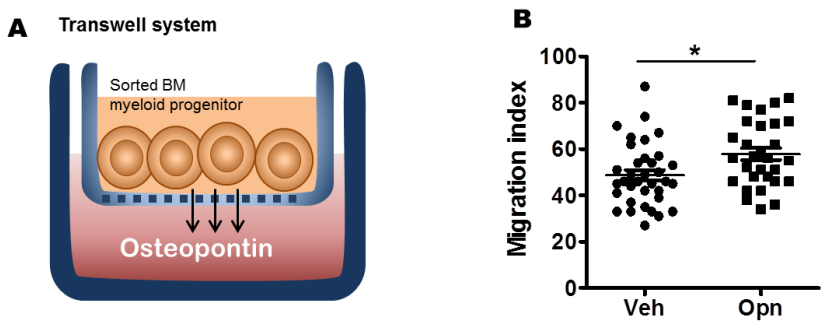

Figure 9. Osteopontin increased migration of myeloid progenitor cells in bone marrow (A) Diagram of transwell system (B) The $2x10^5$ sorted bone marrow LK cells were suspended in the STEMPRO34 complete medium and plated upper well of 24-transwell plate. In the lower well, 2μg/ml osteopontin or vehicle (PBS) were added in STEMPRO34 complete medium and incubated for 18hrs. Then, cells in the lower well were harvested, fixed on the slide glass and Hematoxylin & eosin stained. Migration index was measured by counting the cells in the lower well.

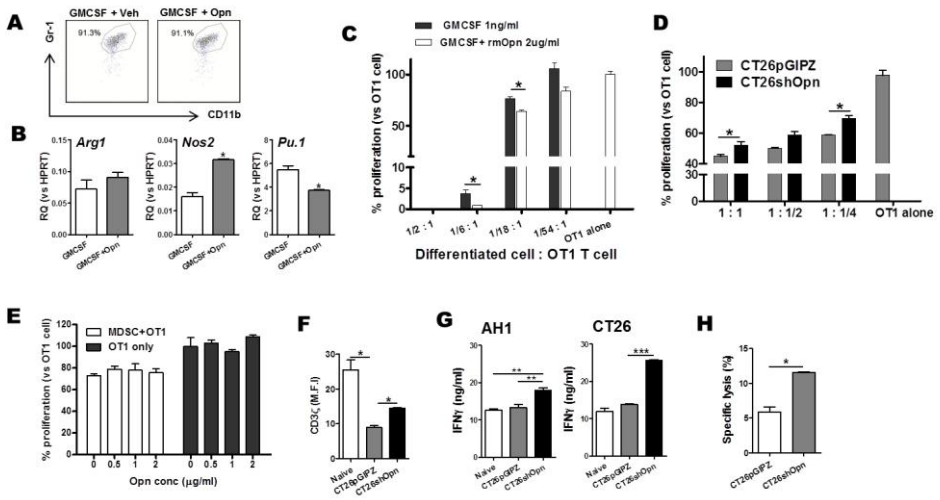

Figure 10. Osteopontin aggravated tumor immunosuppressive environment (A) Sorted splenic LK cells from CT26 tumor bearing mice (3 week) were differentiated with 20ng/ml GMCSF or GMCSF& 2μg/ml osteopontin. The seven days after *in vitro* culture, phenotype of differentiated cells were analyzed by flow cytometry. (B) The mRNA expressions in the differentiated cells were analyzed by quantitative real time PCR. (C) Sorted bone marrow LK from MC38 tumor bearing mice (3 week) were differentiated with 1ng/ml GMCSF or GMCSF& 2μg/ml osteopontin for two days. Then, differentiated cells were co-cultured with OT1 splenocyte (C57BL/6 background) and proliferation of OT1 splenocytes were determined by incorporation of ^{3}H thymidine. (D) Splenic $CD11b^{+}/Gr1^{+}$ MDSCs were purified from CT26pGIPZ or CT26shOpn tumor bearing mice. Then MDSCs were co-cultured with OT1 splenocyte and proliferation of OT1 splenocytes were

determined by incorporation of ^{3}H thymidine. (E) Splenic $CD11b^{+}/Gr1^{+}$ MDSCs were purified from CT26 tumor bearing mice. Then, MDSCs were co-cultured with OT1 splenocyte and osteopontin. The proliferation of OT1 splenocytes were determined by incorporation of ^{3}H thymidine. (F) The expression level of CD3ζ in the $CD3^{+}$ splenocyte of naïve, CT26pGIPZ and CT26shOpn tumor bearing mice (n=3). (G) The splenocytes were re-stimulated with 5μg/ml AH1 peptide or MMC-treated CT26 for five days, and IFNγ concentration in the supernatant were determined by ELISA. (H) AH1 specific *in vivo* target lysis in the 3 week tumor bearing mice (n=3). The data are representative of two independent experiments (*P < 0.05, **P < 0.01, ***P < 0.001)

Part II.

Enhanced antitumor immunotherapeutic effect of B cell-based vaccine transduced with modified adenoviral vector containing type 35 fiber structures

II. 1. Introduction

Recently cancer immunotherapies have been developed to overcome the difficulties associated with chemotherapy, radiotherapy and surgery, which are the most well-known cancer treatment strategies [56]. To this end, dendritic cell-based vaccines were developed to effectively induce robust immune responses against tumor antigens [57-60]. However, there is a need for more efficiently obtained alternative sources of cellular vaccines. In several previous studies, B cells were suggested as a new source of antigen presenting cells for cellular vaccines due to their abundance in the blood and their easy preparation [61-64]. We previously showed that B cells loaded with NKT ligand-loaded B cells into which antigen was introduced by epitope peptide loading or adenoviral vector transduction, could induce strong and long lasting antigen-specific immune responses with the help from activated NKT cells. From these studies, we proposed that if supplemented with NKT ligands, B cell-based vaccines could be taking the place of the DC-based vaccines [61, 62, 65].

Tumor antigen delivery to B cells is another important issue in the induction of strong antitumor immune responses. Adenoviral vector-mediated antigen delivery has been suggested as a useful strategy because a large gene that encodes the antigen of interest can be transferred to the APC, and the adenoviral construct might also act as an adjuvant [66]. Adenovirus serotype 5 (Ad) is a widely used adenoviral vector [67-72]; however, its usage was limited due to the lack of CAR

on APCs, including B cells. To overcome this, we previously reported the combined use of an adenoviral vector and an adapter molecule, CFm40L, to enhance adenoviral gene delivery to B cells [73]. Additionally, adenovirus serotype 35 (Ad35) was recently suggested as alternative adenoviral vector for antigen gene delivery [74-76]. The fiber knob of Ad35 is known to bind the CD46 molecule, which is widely expressed on human leukocytes, for cellular entrance, and this might enhance the adenoviral vector infectivity [77-80]. Furthermore, there have been various challenges involved in the enhancement or specific targeting of adenoviral gene transduction with modified adenoviral vectors [72, 81-83]. Adenovirus type 5, substituted with type 35's fiber knob (Ad-k35), is a vector that was shown to increased infectivity in human cells in either CD46-dependent or independent mechanisms [84].

In our previous study, we established an advanced B cell-based vaccine by enhancing antigen gene delivery to B cells with the modified adenoviral vector Ad-k35 and additional loading with the NKT ligand KBC009 [85, 86]. An Ad-k35HM-transduced B cell-based vaccine elicited strong antigen specific cellular and humoral immune responses, and these responses were further enhanced with additional KBC009 loading (B/Ad-k35HM/KBC009). Moreover, B/Ad-k35HM/KBC009 efficiently suppressed the *in vivo* growth of established tumors in a mouse model [86].

In this study, we investigated various characteristics of Ad-k35HM-transduced and KBC009-loaded B cell-based vaccine. First, we observed increased tumor antigen expression on both human and murine B cells after antigen transduction with Ad-k35HM. The Ad-k35HM transduction induced increases of diverse co-stimulatory molecules on human and murine B cells. Additionally, soluble NKT ligand, KBC-009-loaded B cells effectively activated *in vivo* NKT cells and activated NKT cells trans-activated transferred B cells. Moreover, the vaccine elicited HLA-A2 epitope-specific cytotoxic T cell responses in HLA-A2 Tg mice. These findings suggest that the combined use of an NKT ligand and the modified adenoviral vector Ad-k35 could be appropriate for the preclinical and clinical development of B cell based anticancer immunotherapies.

II. 2. Materials and methods

Mice

BALB/c mice were purchased from the Charles River Laboratories (Seoul, Korea). Chimeric HLA-A2 Tg mice (B6.Cg(CB)-Tg(HLA-A/H2-D)2Enge/Jat, (AAD mice) were purchased from The Jackson Laboratories (Bar Harbor, ME, USA). All mice housed in specific pathogen-free conditions in the Animal Center for Pharmaceutical Research at Seoul National University. The experiments were approved by the International Animal Care and Use Committee of Seoul National University.

Reagent and antibodies

Antibodies for flow cytometry were purchased from either Biolegend (San Diego, CA, USA) or BD Bioscience (San Jose, CA, USA). Anti-mouse B220-FITC, anti-mouse TCRβ-FITC, anti-mouse IA/IE-FITC, anti-mouse CD40-PEcy7, anti-mouse CD80-PE, anti-mouse CD86-PE, anti-mouse CD69-APC, anti-human CD86-PE and anti-human CD40-PEcy7 were purchased from Biolegend. Anti-human CD20-FITC (2H7), anti-human HLA-DP/DQ/DR-FITC, anti-human CD80-PE, anti-human Her2/*neu*-APC, Annexin5-APC and propidium iodine staining solution, recombinant CD1d dimer (Dimer XⅠ) were purchased from BD Bioscience. All microbeads for B cell isolation (anti-mB220 and anti-huCD19) were purchased from Miltenyi Biotec (Bergisch Gladbach, Germany). Nine-mer

$CD8^+$ T cell epitope peptides of Her2/*neu* were purchased from AnyGen (Jeonnam, Korea). The following peptides were used: Her2/*neu* 63-71 (hp63, TYLPTNASL), Her2/*neu* 369-377 (hp369, KIFGSLAFL) and Her2/*neu* 435-443 (hp435, ILHNGAYSL).

Cell lines and culture

The human Her2/*neu*-expressing transfectoma TC1-A2/HM cell line was developed by transfecting pCK-HM into TC1-A2 cells that were kindly provided by Dr. T. C. Wu (The Johns Hopkins University School of Medicine, Baltimore, MD, USA) [87]. Tumor cells were cultured in DMEM medium that was supplemented with 1% penicillin/streptomycin (Lonza, Walkersville, MD, USA) and 10% FBS (GIBCO, Grand Island, NY, USA). Isolated human and murine B cells were cultured in RPMI 1640 medium that was supplemented with 10% FBS, 1% penicillin/streptomycin, 10 mM HEPES, 1 mM sodium pyruvate, 0.1 mM NEAA, and 0.05 mM β-mercaptoethanol.

Adenoviral vectors

All adenoviral vectors were constructed by Prof. CO. Yun (Hanyang University, Seoul, Korea). To construct the adenoviral vector that expressed the Her2/*neu* gene (HM) or the green fluorescent protein (GFP) reporter gene in the E1 region of

adenovirus type 5, we first constructed a pCA14-E1 adenovirus shuttle vector (Microbix, Ontario, Canada) that expressed Her2/*neu* or GFP. The newly generated pCA14-E1-HM or pCA14-E1-GFP vector was co-transformed with an E1/E3-deleted replication-incompetent adenovirus derived from human adenovirus type 5 (E1; SB Verca, University of Fribourg, Switzerland) or an E1/E3-deleted replication-incompetent Ad 5/35 chimeric vector in which a portion of the Ad type 5 fiber was replaced by a portion of the Ad type 35 fiber (Ad-k35) [88], yielding the plasmids pdE1/HM, pdE1/GFP, pdE1-k35/HM and pdE1-k35/GFP. These recombinant plasmids were transfected into human embryonic kidney (HEK) 293 cells to generate AdHM, AdGFP, Ad-k35HM, and Ad-k35GFP. All viruses were obtained as previously described [89].

B cell isolation and B cell-based vaccine preparation

Murine B cells were isolated from total splenocyte using anti-mB220 microbeads. The preparation of human peripheral blood monocyte cells (PBMC) was previously described [90]. B cells from human PBMC were isolated by anti-huCD19 microbead, according to the manufacturer's instructions. Isolated B cells were transduced with the indicated multiplicity of infection (MOI) of adenoviral vectors in a 90 min, 2800 rpm centrifugation step at RT, and the cells were subsequently incubated for an additional 18 hrs. In some experiments, KBC009 was loaded into the prepared B cells for NKT activation, based on our previous studies [61, 62, 91].

Quantitative real-time PCR

Total RNA was isolated by an RNeasy Mini Kit (Qiagen, Valencia, CA, USA) and then reverse-transcribed using amfiRivert Platinum (GenDEPOT, USA). Quantitative real-time PCR was performed on a LightCycler optical system (Roche, California, CA, USA) and SYBR Premix Ex Taq (Takara, Japan). Expression levels of the target genes were calculated relative to *Hprt* expression. The following primers were used: murine *Hprt* sense (AAG ACT TGC TCG AGA TGT CAT GAA), and murine *Hprt* antisense (ATC CAG CAG GTC AGC AAA GAA). human *Hprt* sense (TGG GAC GTC TGG TCC AAG GAT TCA), and human *Hprt* antisense (CCG AAC CCG GGA AAC TGG CCG CC). human *Her2/neu* sense (TTG AAA GGA GGG GTC TTG AT), and human *Her2/neu* antisense (TCT ATC AGT GTG AGA GCC AG).

***In vivo* NKT activation and *in vivo* transferred B cell analysis**

The α-galactosyl ceramide (α-GC) derivative KBC009 was used as an NKT ligand.[32] Purified B cells from murine splenocytes were transduced with 100 MOI of the indicated HM-encoding adenoviral vectors and subsequently loaded with 1μg/ml of KBC009 or vehicle. Untreated B cells were used as controls. After an overnight incubation, $2x10^6$ manipulated B cells were intravenously injected into mice. Four hours later, the mice were sacrificed and CD69 expression on splenic

NKT cells in was analyzed by flowcytometry on a FACS Calibur (BD Biosciences). Additionally after a four-hr treatment with the manipulated B cells, the serum levels of IFNγ and IL4 were determined by ELISA (BD Biosciences) according to the manufacturer's instructions. For analysis of activation markers on transferred B cells, $2x10^6$ cells of 10 μM of CFSE-labeled B or B/KBC009 were injected to mice. Twenty-four hours later, $CFSE^+$ B cells in murine splenocytes were analyzed by flow cytometry.

Evaluation of HLA-A2 epitope specific cytotoxic T cell response

AAD mice immunized with indicated B cell-based vaccine. 9 days after immunization, mice were sacrificed and splenocyte were re-stimulated with an HLA-A2-epitope peptide of Her2/*neu* or MMC-treated TC1-A2/HM cells for 2 days. IFNγ production was measured by ELISPOT assay (BD bioscience) according to the manufacturer's instructions. Additionally, IFNγ levels on the culture supernatant were determined by ELISA (BD Biosciences) according to the manufacturer's instructions.

Statistics

The data are shown as the means ± SEM, and statistical significance was analyzed with Graph Pad Prism software. A two-tailed Student's *t*-test was used to compare differences between two groups. *p* values <0.05 were considered significant at a 95% confidence interval.

II. 3. Results

Expression kinetics of Her2/*neu* following adenoviral vector transduction

For the establishment of B cell-based vaccines, both adenoviral vector transduction into B cells and proper expression of the transduced antigen is crucial to the generation of antigen-specific immune responses. To test this, we introduced a truncated form of the breast cancer antigen, Her2/*neu* (HM) into Ad-k35 vectors (Ad-k35HM). An HM encoding adenovirus serotype 5 (AdHM) was used as a control. We transduced these HM-encoding adenoviral vectors to human B cells and evaluated HM mRNA expression by real time PCR at various time points after the adenoviral vector infections. B/Ad-k35HM rapid induced a 60 fold increase in mRNA expression over that of B/AdHM at 12 hr; however the expression level decreased at 18 hrs in the B/Ad-k35HM-transduced cells while those transduced with B/AdHM maintained a constant mRNA expression level (Figure 11A). Although the HM mRNA expression increased transiently following Ad-k35HM transduction, we observed that the HM protein level gradually increased until 48 hrs after adenoviral vector transduction (Figure 11B).

To test these B cell-based vaccines in mice, we examined whether Ad-k35HM could efficiently transfer adenoviral genes to murine B cells. The trend of HM mRNA expression in murine B cells was similar to that of human B cells. Specifically, a time-dependent increase was observed until 12 hr, which decreased by 18 hr, however, gene expression was greatly enhanced by Ad-k35HM, such that

30-fold and 240-fold increases were observed at 6 hr and 12 hr, respectively, compared to the AdHM-transfected cells (Figure 11C).

Expression of various co-stimulatory molecules on adenoviral vector-transduced human and murine B cells

To address characteristics of the adenoviral vector transduced B cell, we analyzed diverse co-stimulatory molecules on human and murine B cells after adenoviral vector transduction. We found higher expression levels of CD86, CD80 and MHC class II on the surfaces of B/Ad-k35HM-transduced human B cells than on B/AdHM-transduced cells. The CD40 expression on the cells of the B/Ad-k35HM group was also higher than that of the B/AdHM group, although it was indistinguishable from that of the B cell-only group (Figure 12A). In murine B cells, CD86 expression was transiently higher in Ad-k35HM transduced B cells at 18 hr-post transduction than that of B cells transduced with AdHM. Additionally, CD80 and CD40 expressions were slightly increased by Ad-k35 adenoviral vector transduction to B cells than that of AdHM transduced cells while MHC ClassII molecule expression was not changed (Figure 12B). Collectively, these data indicated that the substitution of the Ad5 fiber knob by the Ad35 fiber knob enhanced adenoviral gene delivery and more effectively activated the both human and murine B cells.

Soluble NKT ligand, KBC009 loaded-B cells directly activated NKT cell *in vivo*; NKT cells subsequently stimulated transferred B cells and activated them to become immunogenic antigen presenting cells

After interacting with NKT cells via the loaded NKT ligand on B cells, B cells can become powerful antigen presenting cells and induce a wide spectrum of immune responses [65]. KBC009, the α-galactosyl ceramide (α–GC) derivative that demonstrated improved solubility, was found to activate NKT cells *in vitro* and to exhibit potent adjuvant effects *in vivo* [85]. Therefore, we determined whether KBC009-loaded B cells could stimulate NKT cells *in vivo*. As expected, NKT cells from mice treated with KBC009-loaded B cells up-regulated the early activation indicator CD69, regardless of the adenoviral vector transduction (Figure 13A and Figure 14B). The IFNγ and IL4 levels were elevated in the sera from mice treated with KBC009-loaded B cells at 4 hr post-treatment (Figure 13B). NKT cells are generally considered to be the main source of IFNγ and IL4 within 4 hours of stimulation. As expected, we found that NKT cells were the main cellular source of these cytokines by intracellular cytokine staining analysis (Figure 14A). Adenoviral vectors transduction of B cells did not influence *in vivo* NKT activation. Furthermore, *in vivo*-activated NKT cells induce increased expression levels of CD80, CD86, MHC class I and MHC class II on transferred B cells (Figure 13C). These data suggest that KBC009-loaded B cells can directly activate NKT cells *in vivo*; NKT cells can subsequently stimulate B cells and activate them to become

immunogenic APCs that can induce overall immune responses, as previously described [61, 62, 65].

Induction of human HLA-A2 epitope-restricted $CD8^+$ T cells immune response by an Ad-k35HM transduced B cell-based vaccine

Next, we tested whether the Ad-k35HM-transduced NKT ligand-loaded B cell-based vaccines could also induce human MHC molecule-restricted $CD8^+$ T cell immune responses. To ascertain this, we used transgenic mice that expressed a hybrid class I MHC gene (AAD mice) that encoded the epitope peptide-binding alpha-1 and alpha-2 domains of the human HLA-A2.1 gene and the transmembrane and cytoplasmic alpha-3 domains of the murine $H\text{-}2D^d$ gene. These mice have been widely used for evaluations of human HLA-A0201-restricted cytotoxic T cell responses [92, 93]. The AAD mice were immunized with Ad-k35HM-transduced B cell-based vaccines and after 9 days, the splenocytes were re-stimulated *ex vivo* with either two Her2/*neu*-specific, and HLA-A2-restricted nine-mer peptides (a mixture of hp363 and hp435) or TC1-A2/HM murine tumor cells, which express both HLA-A2 and Her2/*neu*. As shown in Figures 15A and 15B, re-stimulation with either the peptides or TC1-A2/HM significantly increased the numbers of $IFN\gamma^+$ spots from B/Ad-k35HM/KBC009 group splenocytes. B/Ad-k35HM group splenocytes also produce IFNγ but at relatively lower levels than the B/Ad-k35HM/KBC009 group cells. A similar result was observed when the IFNγ

concentrations were measured in the TC1-A2/HM re-stimulated culture supernatants (Figure 15C). These data imply that B/Ad-k35HM/KBC009 effectively elicited HLA-A2-restricted antigen-specific CTL responses.

II. 4. Discussion

In this report, we described various characteristics and HLA-A2 specific antitumor immune response of advanced B cell-based anticancer therapeutic vaccine. The tumor antigen delivery was significantly enhanced by Ad-k35HM transduction. Moreover, various co-stimulatory molecules were up-regulated by Ad-k35HM transduction. In addition, soluble NKT ligand, KBC-009-loaded B cells effectively activated *in vivo* NKT cells and activated NKT cells transactivated transferred B cells. Moreover, the vaccine effectively elicited HLA-A2 epitope-specific cytotoxic T cell responses in HLA-A2 Tg mice.

The proper generation of strong immune responses against tumor antigen is required for successful clinical tumor immunotherapy outcomes. Traditional vaccination strategies that are administered against infectious diseases, such as co-injections of antigen or antigen-encoding DNA with an adjuvant, have been adapted in early cancer therapeutic vaccine development. These methods are simple and cost effective, but unfortunately have been ineffective as solid cancer treatments because they could not provide the necessary in situ APCs stimulation that was required for the priming of antigen-specific immune responses [56]. Recently, tumor antigen-expressing, *ex vivo*-differentiated, mature autologous dendrite cell-based vaccines have been developed and have been shown to effectively induce tumor antigen-specific immunity. However, expensive and labor-intensive *ex vivo* manipulations are required to generate DC-based vaccines,

although these promise powerful therapeutic antitumor immunity [58-60]. Therefore, we, along with others, suggested B cells as an alternative source of APC-based vaccines that were easily obtainable from human blood and did not require *ex vivo* maturation for cellular vaccine preparation [61, 63, 64]. Previously, we showed that NKT ligand-loaded on and antigen introduced by epitope peptide loading or adenoviral vector transduction to B cells could generate a broad spectrum of antigen-specific immune responses [61, 65].

Strategies of tumor antigen delivery to B cells are another important issue in the clinical development of B cell-based vaccines. Although exogenous epitope peptide loading is simple and effective, this strategy is limited due to the various patient MHC haplotypes [59]. To overcome this problem, whole antigen introduction into B cells by transduction with an antigen gene-encoding serotype-5 based replication-incompetent adenoviral vector was suggested [62]. The adenovarally transduced tumor antigen could be processed within B cells and subsequently presented on the B cell surface by most MHC molecules. However, adenovirus-5 based adenoviral vectors have low antigen transduction efficiency due to the lack of CAR molecules expression on APCs such as B cells. To overcome this limitation, we previously reported the combined use of an adenoviral vector and an adapter molecule, CFm40L; this combination demonstrated enhanced transduction efficacy and subsequent antitumor immune responses from B cell-based vaccines [73]. However, it remains unknown whether this combination induces undesirable

immune responses against the chimeric protein, CFm40L and consequent toxicities. Therefore, there has been a demand for alternative adenoviral vectors to allow more efficient delivery of tumor antigen genes to antigen presenting cells. Adenovirus serotype 35 (Ad35) was recently suggested because it can easily deliver genes through CD46 molecules expressed on most human leukocytes [78, 79]. Repeated vaccination with Ad35 induced stronger memory CD8 T cell responses than vaccination with Ad5, indicating that Ad35 could be a useful alternative adenoviral vector which could replace Ad5 [94]. Also, there are various challenges in the construction of modified adenoviral vectors for transduction enhancement or specific *in vivo* targeting. In this study, we designed a replicate-incompetent Ad5-based modified adenoviral vector containing a substituted Ad35 fiber knob (Ad-k35) to take advantage of Ad35's infectivity. This approach enabled us to anticipate the enhanced transduction efficiency by the Ad-k35 adenoviral vector. As expected, compared to AdHM, the tumor antigen-introduced Ad-k35HM (Ad-k35/HM) showed superior infectivity in B cells and subsequently enhanced the antigen expression on B cells (Figures 11). Ad-k35HM transduced B cells up-regulated various co-stimulatory molecules including CD80, CD86, CD40 and MHC classII (Figure 12). Soluble NKT ligand, KBC009-loaded B cell directly activate NKT cells *in vivo* and activated NKT cells trans-activated transferred B cells (Figure 13 and Figure 14). Moreover, Ad-k35HM transduced B cell-based vaccine efficiently induced HLA-A2 specific cytotoxic T cell responses in the

AAD mice (Figure 15). Collectively, these data indicate that the Ad-k35 vector is appropriate for B cell-based cancer therapeutic vaccine development.

In this study we investigated the development of advanced B cell based vaccine with an Ad-k35 adenoviral vector which enhances antigen delivery to B cells. We hypothesized that antigen transfer enhancement with an Ad-k35adenoviral vector might elicit enhanced overall antigen-specific immune responses and subsequently maximize the cancer therapeutic effects of B cell-based vaccines. To ascertain this, we introduced a truncated form of well-known tumor antigen Her2/*neu* to Ad-k35 adenoviral vector (Ad-k35/HM) to enhance the adenoviral antigen transfer. As expected, the Ad-k35 adenoviral vector greatly increased the antigen transduction efficiency in human B cells (Figure 11A and 11B) [84]. Moreover, enhanced antigen transfer to human B cells subsequently elevated expression of several co-stimulatory molecules (Figures 12A) suggesting that transduced adenoviral vector might act as an adjuvant [66]. However, it is unclear if the increased expression was due to the substituted Ad35 fiber knob or to the enhanced adenoviral vector delivery to B cells. Because the intracellular signaling events triggered by CD46 ligation are still unknown, the changes in the intracellular events induced by ligation of the k35 fiber knob-CD46 on human B cells need to be investigated in future studies.

Despite the rare expression of CD46 on murine leukocytes [95], Ad-k35HM also improved the transduction efficiency in murine B cells (Figure 11C) which means

that its underlying mechanism is independent on CD46. Recently, several studies reported that the adenovirus serotype 35 could enter host cells by both CD46-dependent and independent mechanisms [84]; thus further studies might be needed to determine the mechanisms of CD46-independent entrance.

As well as enhancing antigen transduction into B cells, the co-presentation of NKT ligands and processed antigen on same B cells is crucial to the generation of antigen-specific immune responses of B cell based vaccines [61]. Although α-GC is a well-known NKT ligand, its poor solubility needs to be improved upon for the clinical development of NKT ligand-loaded B cell-based vaccines. Therefore, we used KBC009, a water-soluble derivative of α-GC [85]. The KBC009-loaded B cells effectively activated NKT cells *in vivo*, regardless of adenoviral vector transductions (Figure 13A and 13B and Figure 14). Moreover, activated-NKT cells can subsequently stimulate B cells and activate them to become immunogenic APCs that can induce overall immune responses (Figure 13C). These data implicate KBC009-loaded, Ad-k35HM-transduced B cell-based vaccines could promote overall in vivo antigen-specific immunity, which includes NKT cell activation.

Moreover, either B/Ad-k35HM or B/Ad-k35HM/KBC009 vaccination of AAD mice effectively induced HLA-A2 antigen-restricted $CD8^+$ T cell immune responses (Figure 15) implying that these B cell-based vaccines could also be effective in human immune system.

Taken together, the present study proposes B/Ad-k35HM/KBC009 as a novel and advanced B cell-based therapeutic vaccine regimen for the treatment of Her2/neu-expressing solid cancers. In addition, NKT ligand-loaded, Ad-k35 adenoviral vector tumor antigen-transduced B cells could be useful in the development of therapeutic cell based vaccines for various cancers.

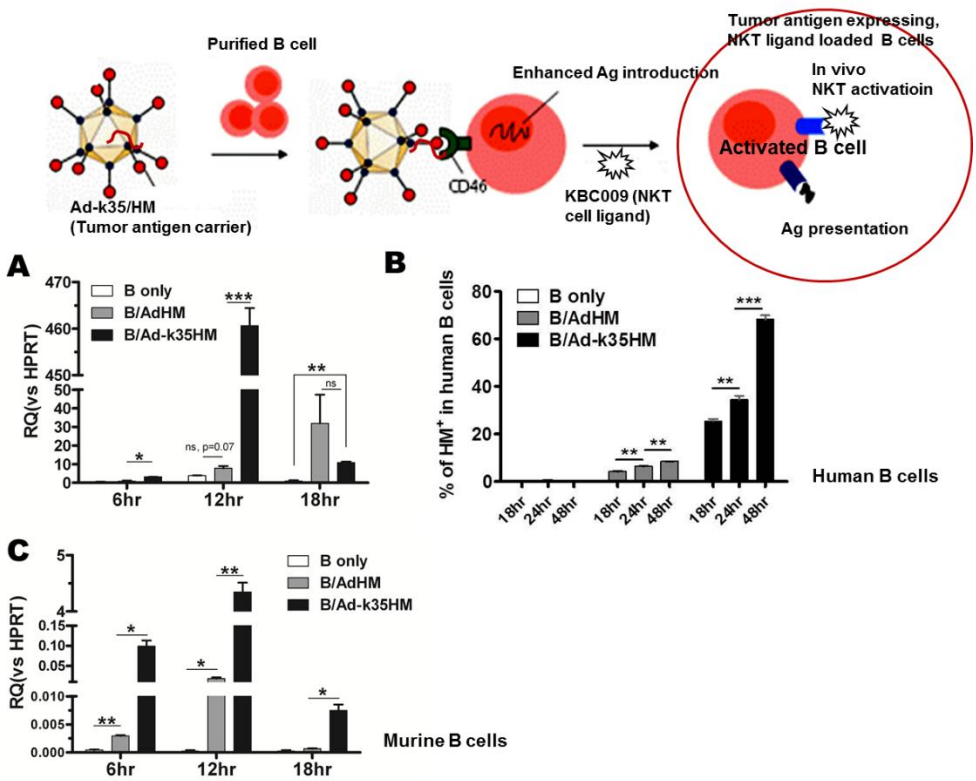

Figure 11. Expression kinetics of Her2/neu following adenoviral vector transduction (A) Two hundred MOI of AdHM or Ad-k35HM were transduced into purified human B cells and HM mRNA expression was measured by qPCR. (B) One hundred MOI of AdHM or Ad-k35HM was transduced into purified human B cells. The expression kinetics of the HM protein was analyzed by flow cytometry at 18, 24 and 48 hours after adenoviral vector transduction. (C) One hundred MOI of AdHM or Ad-k35HM was transduced into purified murine B cells, and HM mRNA expression was measured by qPCR. The data are representative of two independent experiments (*P < 0.05, **P < 0.01, ***P < 0.001).

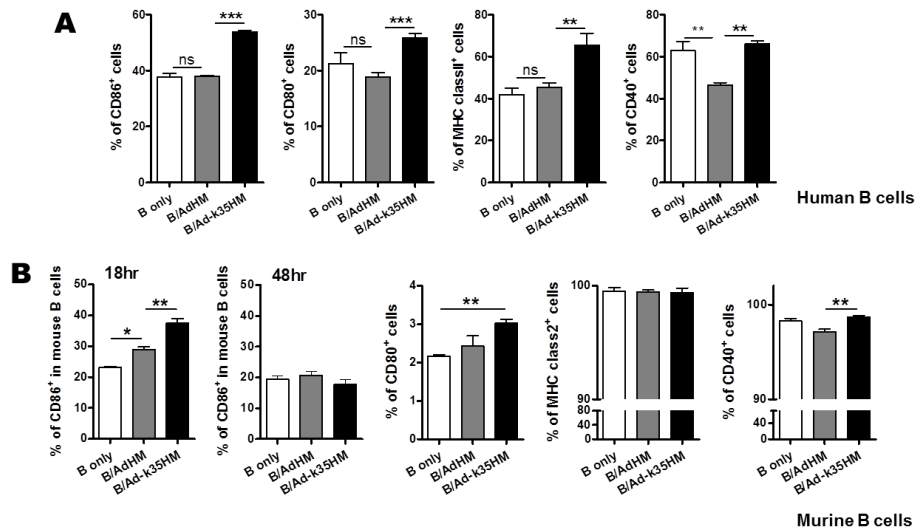

Figure 12. Expression of co-stimulatory molecules on adenoviral vector-transduced human and murine B cells One hundred MOI of AdHM or Ad-k35HM was transduced into purified (A) human B cells or (B) murine B cells. After 24 hr of incubation, the expression levels of CD86, CD80, MHC class II, and CD40 were analyzed by flow cytometry (*P < 0.05, **P < 0.01, ***P < 0.001).

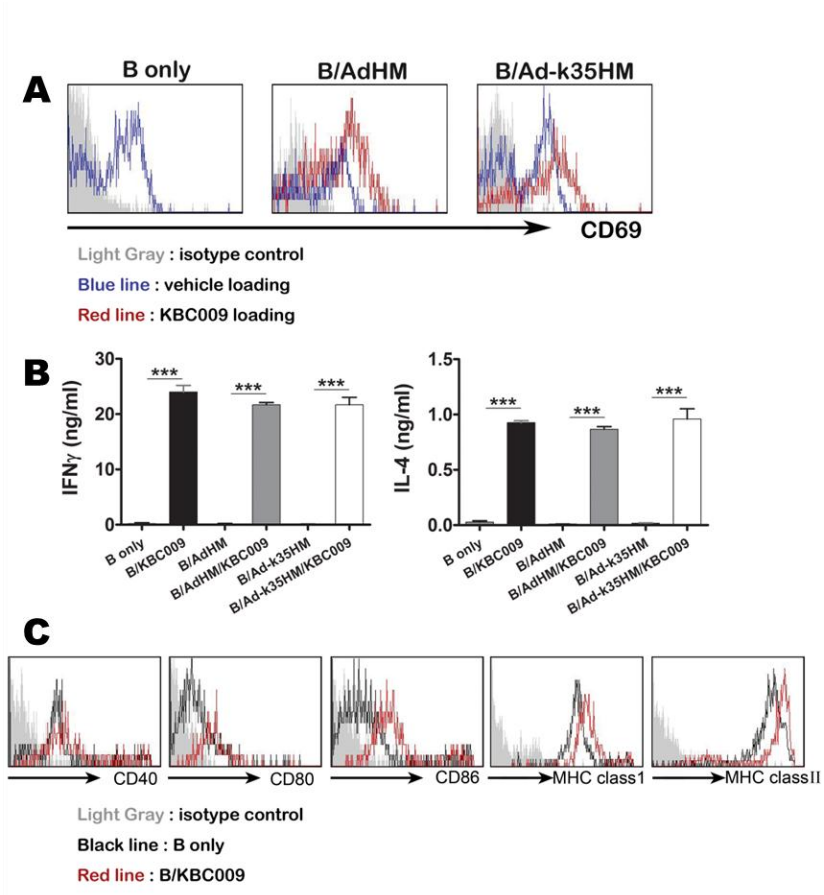

Figure 13. Direct *in vivo* activation of NKT cells through KBC009 loaded B cells and activation of transferred B cells by activated NKT cells (A) The indicated B cell-based vaccines were injected i.v. into mice. At 4 hrs post-injection, CD69 expression on the $CD1d^{+}/TCR\beta^{+}$ NKT cells in total murine splenocyte were analyzed by flow cytometry. (B) IFNγ and IL-4 in the sera from the indicated B cell-based vaccine-immunized mice was quantified by ELISA at 4 hr post-injection (*P < 0.05, **P < 0.01, ***P < 0.001). (C) The indicated B cell-based vaccines were injected i.v. into mice. Activation markers on transferred B cells were analyzed by flow cytometry at 24 hr post-injection.

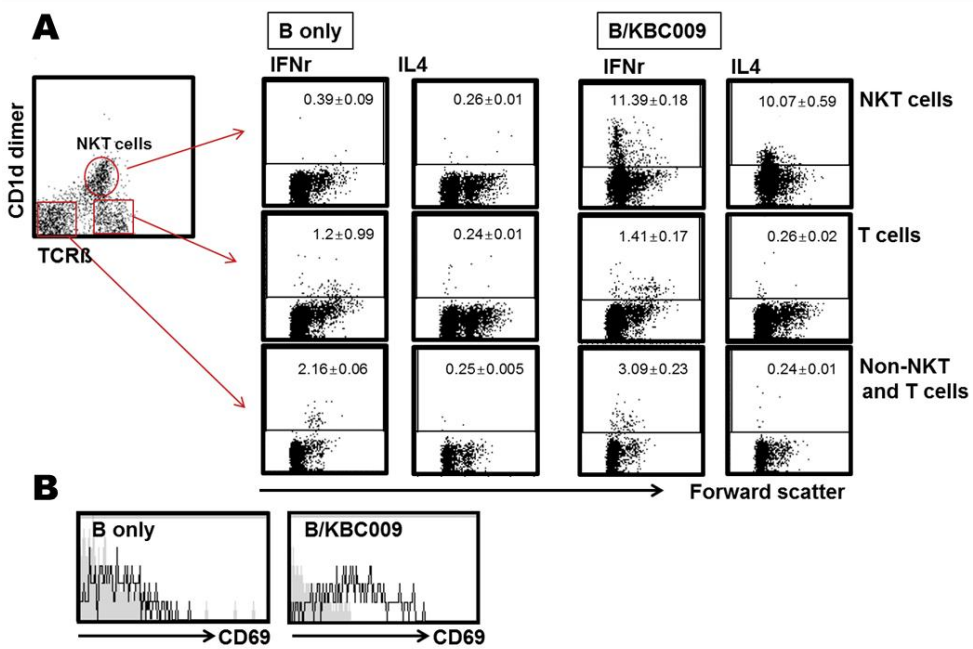

Figure 14. Activation of NKT cells following KBC009 loaded B cell transfer (A) Purified murine B cells or KBC009-loaded murine B cells were injected i.v. into mice. At 4 hr post-injection, the IFNs- or IL-4-secreting cells among the total murine splenocyte population were analyzed by intracellular cytokine staining. (B) CD69 expression on the $CD1d^{+}/TCR6^{+}$ NKT cell fraction of total murine splenocytes was analyzed by flow cytometry.

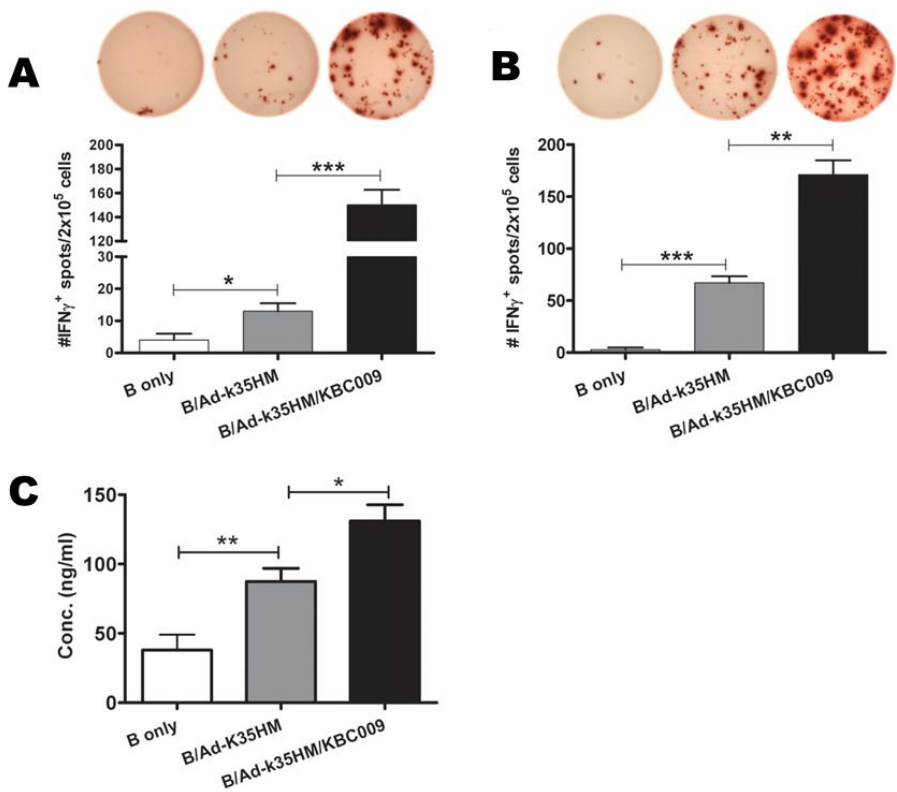

Figure 15. Induction of human HLA-A2 epitope-restricted cytotoxic immunity by Ad-k35HM-transduced B cell-based vaccine (A) On day 0, AAD mice were immunized with 2 x 10^6 cells containing the indicated B cell-based vaccine. Nine days later, splenocytes from the immunized mice were re-stimulated with an HLA-A2-epitope peptide of Her2/*neu* or (B) MMC-treated TC1-A2/HM cells for 2 days. IFNγ production was measured with an ELISPOT assay. (C) IFNγ in the supernatant from TC1-A2/HM re-stimulated cells was quantified by ELISA (*P < 0.05, **P < 0.01, ***P < 0.001).

References

1. Cortez-Retamozo, V., et al., *Origins of tumor-associated macrophages and neutrophils.* Proceedings of the National Academy of Sciences, 2012. **109**(7): p. 2491-2496.
2. Galdiero, M.R., et al., *Tumor associated macrophages and neutrophils in cancer.* Immunobiology, 2013. **218**(11): p. 1402-10.
3. Murdoch, C., et al., *The role of myeloid cells in the promotion of tumour angiogenesis.* Nature Reviews Cancer, 2008. **8**(8): p. 618-631.
4. Youn, J.I., et al., *Subsets of myeloid-derived suppressor cells in tumor-bearing mice.* J Immunol, 2008. **181**(8): p. 5791-802.
5. Lindau, D., et al., *The immunosuppressive tumour network: myeloid-derived suppressor cells, regulatory T cells and natural killer T cells.* Immunology, 2013. **138**(2): p. 105-115.
6. Liu, C., et al., *Expansion of spleen myeloid suppressor cells represses NK cell cytotoxicity in tumor-bearing host.* Blood, 2007. **109**(10): p. 4336-42.
7. Bronte, V., *Myeloid-derived suppressor cells in inflammation: uncovering cell subsets with enhanced immunosuppressive functions.* Eur J Immunol, 2009. **39**(10): p. 2670-2.
8. Corzo, C.A., et al., *Mechanism Regulating Reactive Oxygen Species in Tumor-Induced Myeloid-Derived Suppressor Cells.* The Journal of Immunology, 2009. **182**(9): p. 5693-5701.
9. Ostrand-Rosenberg, S. and P. Sinha, *Myeloid-Derived Suppressor Cells: Linking Inflammation and Cancer.* The Journal of Immunology, 2009. **182**(8): p. 4499-4506.
10. Rodriguez, P.C., et al., *Arginase I-Producing Myeloid-Derived Suppressor Cells in Renal Cell Carcinoma Are a Subpopulation of Activated Granulocytes.* Cancer Research, 2009. **69**(4): p. 1553-1560.
11. Nagaraj, S., et al., *Mechanism of T Cell Tolerance Induced by Myeloid-*

Derived Suppressor Cells. The Journal of Immunology, 2010. **184**(6): p. 3106-3116.

12. Ostrand-Rosenberg, S., *Myeloid-derived suppressor cells: more mechanisms for inhibiting antitumor immunity.* Cancer Immunology, Immunotherapy, 2010. **59**(10): p. 1593-1600.
13. Lechner, M.G., et al., *Functional characterization of human Cd33+ and Cd11b+ myeloid-derived suppressor cell subsets induced from peripheral blood mononuclear cells co-cultured with a diverse set of human tumor cell lines.* J Transl Med, 2011. **9**: p. 90.
14. Obermajer, N., et al., *PGE2-Induced CXCL12 Production and CXCR4 Expression Controls the Accumulation of Human MDSCs in Ovarian Cancer Environment.* Cancer Research, 2011. **71**(24): p. 7463-7470.
15. Youn, J.I., et al., *Epigenetic silencing of retinoblastoma gene regulates pathologic differentiation of myeloid cells in cancer.* Nat Immunol, 2013. **14**(3): p. 211-20.
16. Qu, P., C. Yan, and H. Du, *Matrix metalloproteinase 12 overexpression in myeloid lineage cells plays a key role in modulating myelopoiesis, immune suppression, and lung tumorigenesis.* Blood, 2011. **117**(17): p. 4476-4489.
17. Park, Y.J., et al., *Tumor Microenvironmental Conversion of Natural Killer Cells into Myeloid-Derived Suppressor Cells.* Cancer Research, 2013. **73**(18): p. 5669-5681.
18. Sawanobori, Y., et al., *Chemokine-mediated rapid turnover of myeloid-derived suppressor cells in tumor-bearing mice*. Blood, 2008. **111**(12): p. 5457-5466.
19. Morales, J.K., et al., *GM-CSF is one of the main breast tumor-derived soluble factors involved in the differentiation of CD11b-Gr1- bone marrow progenitor cells into myeloid-derived suppressor cells.* Breast Cancer Research and Treatment, 2009. **123**(1): p. 39-49.

20. Shojaei, F., et al., *G-CSF-initiated myeloid cell mobilization and angiogenesis mediate tumor refractoriness to anti-VEGF therapy in mouse models.* Proceedings of the National Academy of Sciences, 2009. **106**(16): p. 6742-6747.
21. Blagosklonny, M.V., et al., *Tumor-Derived G-CSF Facilitates Neoplastic Growth through a Granulocytic Myeloid-Derived Suppressor Cell-Dependent Mechanism.* PLoS ONE, 2011. **6**(11): p. e27690.
22. Sevko, A. and V. Umansky, *Myeloid-derived suppressor cells interact with tumors in terms of myelopoiesis, tumorigenesis and immunosuppression: thick as thieves.* J Cancer, 2013. **4**(1): p. 3-11.
23. Balducci, L. and C. Hardy, *High proliferation of granulocyte-macrophage progenitors in tumor-bearing mice.* Cancer Res, 1983. **43**(10): p. 4643-7.
24. O'Malley, D.P., *Benign extramedullary myeloid proliferations.* Modern Pathology, 2007. **20**(4): p. 405-415.
25. Swirski, F.K., et al., *Identification of Splenic Reservoir Monocytes and Their Deployment to Inflammatory Sites.* Science, 2009. **325**(5940): p. 612-616.
26. Wang, K.X. and D.T. Denhardt, *Osteopontin: Role in immune regulation and stress responses.* Cytokine & Growth Factor Reviews, 2008. **19**(5-6): p. 333-345.
27. Koh, A., et al., *Role of osteopontin in neutrophil function.* Immunology, 2007. **122**(4): p. 466-475.
28. McAllister, S.S., et al., *Systemic Endocrine Instigation of Indolent Tumor Growth Requires Osteopontin.* Cell, 2008. **133**(6): p. 994-1005.
29. Behera, R., et al., *Activation of JAK2/STAT3 signaling by osteopontin promotes tumor growth in human breast cancer cells.* Carcinogenesis, 2009. **31**(2): p. 192-200.
30. Lee, J.M., et al., *The restoration of myeloid-derived suppressor cells as*

functional antigen-presenting cells by NKT cell help and all-trans-retinoic acid treatment. Int J Cancer, 2012. **131**(3): p. 741-51.

31. Kim, R., *Tumor-Driven Evolution of Immunosuppressive Networks during Malignant Progression.* Cancer Research, 2006. **66**(11): p. 5527-5536.
32. Sica, A., et al., *Origin and Functions of Tumor-Associated Myeloid Cells (TAMCs).* Cancer Microenvironment, 2011. **5**(2): p. 133-149.
33. Kim, Y.S., et al., *Functional changes in myeloid-derived suppressor cells (MDSCs) during tumor growth: FKBP51 contributes to the regulation of the immunosuppressive function of MDSCs.* J Immunol, 2012. **188**(9): p. 4226-34.
34. Swirski, F.K., et al., *Identification of splenic reservoir monocytes and their deployment to inflammatory sites.* Science, 2009. **325**(5940): p. 612-6.
35. Cortez-Retamozo, V., et al., *Angiotensin II drives the production of tumor-promoting macrophages.* Immunity, 2013. **38**(2): p. 296-308.
36. Bellahcene, A., et al., *Small integrin-binding ligand N-linked glycoproteins (SIBLINGs): multifunctional proteins in cancer.* Nat Rev Cancer, 2008. **8**(3): p. 212-26.
37. Denhardt, D.T. and M. Noda, *Osteopontin expression and function: role in bone remodeling.* J Cell Biochem Suppl, 1998. **30-31**: p. 92-102.
38. Reinholt, F.P., et al., *Osteopontin--a possible anchor of osteoclasts to bone.* Proc Natl Acad Sci U S A, 1990. **87**(12): p. 4473-5.
39. Ashkar, S., et al., *Eta-1 (osteopontin): an early component of type-1 (cell-mediated) immunity.* Science, 2000. **287**(5454): p. 860-4.
40. Nagai, S., et al., *Comprehensive gene expression profile of human activated T(h)1- and T(h)2-polarized cells.* Int Immunol, 2001. **13**(3): p. 367-76.
41. Liersch, R., et al., *Osteopontin is a prognostic factor for survival of acute myeloid leukemia patients.* Blood, 2012. **119**(22): p. 5215-5220.

42. Agrawal, D., et al., *Osteopontin identified as colon cancer tumor progression marker.* C R Biol, 2003. **326**(10-11): p. 1041-3.
43. Said, H.M., et al., *Response of the plasma hypoxia marker osteopontin to in vitro hypoxia in human tumor cells.* Radiother Oncol, 2005. **76**(2): p. 200-5.
44. Chen, R.X., et al., *Osteopontin, a single marker for predicting the prognosis of patients with tumor-node-metastasis stage I hepatocellular carcinoma after surgical resection.* J Gastroenterol Hepatol, 2010. **25**(8): p. 1435-42.
45. Rangaswami, H., A. Bulbule, and G.C. Kundu, *Osteopontin: role in cell signaling and cancer progression.* Trends Cell Biol, 2006. **16**(2): p. 79-87.
46. Luo, X., et al., *Osteopontin stimulates preneoplastic cellular proliferation through activation of the MAPK pathway.* Mol Cancer Res, 2011. **9**(8): p. 1018-29.
47. Zhou, Y., et al., *Osteopontin expression correlates with melanoma invasion.* J Invest Dermatol, 2005. **124**(5): p. 1044-52.
48. Sun, B.S., et al., *Lentiviral-mediated miRNA against osteopontin suppresses tumor growth and metastasis of human hepatocellular carcinoma.* Hepatology, 2008. **48**(6): p. 1834-42.
49. Wai, P.Y., *Osteopontin silencing by small interfering RNA suppresses in vitro and in vivo CT26 murine colon adenocarcinoma metastasis.* Carcinogenesis, 2005. **26**(4): p. 741-751.
50. Grassinger, J., et al., *Thrombin-cleaved osteopontin regulates hemopoietic stem and progenitor cell functions through interactions with 9 1 and 4 1 integrins.* Blood, 2009. **114**(1): p. 49-59.
51. Nilsson, S.K., et al., *Osteopontin, a key component of the hematopoietic stem cell niche and regulator of primitive hematopoietic progenitor cells.* Blood, 2005. **106**(4): p. 1232-9.

52. Kalluri, H.S.G. and R.J. Dempsey, *Osteopontin increases the proliferation of neural progenitor cells.* International Journal of Developmental Neuroscience, 2012. **30**(5): p. 359-362.
53. Rollo, E.E., D.L. Laskin, and D.T. Denhardt, *Osteopontin inhibits nitric oxide production and cytotoxicity by activated RAW264.7 macrophages.* J Leukoc Biol, 1996. **60**(3): p. 397-404.
54. Iwata, M., et al., *Human marrow stromal cells activate monocytes to secrete osteopontin, which down-regulates Notch1 gene expression in CD34+ cells.* Blood, 2004. **103**(12): p. 4496-502.
55. Cheng, P., et al., *Effects of Notch signaling on regulation of myeloid cell differentiation in cancer.* Cancer Res, 2013.
56. Rosenberg, S.A., J.C. Yang, and N.P. Restifo, *Cancer immunotherapy: moving beyond current vaccines.* Nat Med, 2004. **10**(9): p. 909-15.
57. Schreurs, M.W., et al., *Generation and functional characterization of mouse monocyte-derived dendritic cells.* Eur J Immunol, 1999. **29**(9): p. 2835-41.
58. Elkord, E., et al., *Human monocyte isolation methods influence cytokine production from in vitro generated dendritic cells.* Immunology, 2005. **114**(2): p. 204-12.
59. Gilboa, E., *DC-based cancer vaccines.* J Clin Invest, 2007. **117**(5): p. 1195-203.
60. Palucka, K. and J. Banchereau, *Cancer immunotherapy via dendritic cells.* Nature Reviews Cancer, 2012. **12**(4): p. 265-277.
61. Chung, Y., *CD1d-Restricted T Cells License B Cells to Generate Long-Lasting Cytotoxic Antitumor Immunity In vivo.* Cancer Research, 2006. **66**(13): p. 6843-6850.
62. Kim, Y.-J., et al., *α-Galactosylceramide-loaded, antigen-expressing B cells prime a wide spectrum of antitumor immunity.* International Journal of

Cancer, 2008. **122**(12): p. 2774-2783.

63. Schultze, J.L., S. Grabbe, and M.S. von Bergwelt-Baildon, *DCs and CD40-activated B cells: current and future avenues to cellular cancer immunotherapy.* Trends Immunol, 2004. **25**(12): p. 659-64.

64. Schultze, J.L., et al., *CD40-activated human B cells: an alternative source of highly efficient antigen presenting cells to generate autologous antigen-specific T cells for adoptive immunotherapy.* J Clin Invest, 1997. **100**(11): p. 2757-65.

65. Kim, Y.-J., et al., *NKT ligand-loaded, antigen-expressing B cells function as long-lasting antigen presenting cells in vivo.* Cellular Immunology, 2011. **270**(2): p. 135-144.

66. Appledorn, D.M., et al., *Adenovirus vector-induced innate inflammatory mediators, MAPK signaling, as well as adaptive immune responses are dependent upon both TLR2 and TLR9 in vivo.* J Immunol, 2008. **181**(3): p. 2134-44.

67. Brough, D.E., et al., *A gene transfer vector-cell line system for complete functional complementation of adenovirus early regions E1 and E4.* J Virol, 1996. **70**(9): p. 6497-501.

68. Xiang, Z.Q., et al., *A replication-defective human adenovirus recombinant serves as a highly efficacious vaccine carrier.* Virology, 1996. **219**(1): p. 220-7.

69. Shiver, J.W., et al., *Replication-incompetent adenoviral vaccine vector elicits effective anti-immunodeficiency-virus immunity.* Nature, 2002. **415**(6869): p. 331-5.

70. Tan, Y., et al., *Protective immunity evoked against anthrax lethal toxin after a single intramuscular administration of an adenovirus-based vaccine encoding humanized protective antigen.* Hum Gene Ther, 2003. **14**(17): p. 1673-82.

71. Shiver, J.W. and E.A. Emini, *Recent advances in the development of HIV-1 vaccines using replication-incompetent adenovirus vectors.* Annu Rev Med, 2004. **55**: p. 355-72.
72. Lasaro, M.O. and H.C. Ertl, *New insights on adenovirus as vaccine vectors.* Mol Ther, 2009. **17**(8): p. 1333-9.
73. Kim, Y.-S., et al., *CD40-Targeted Recombinant Adenovirus Significantly Enhances the Efficacy of Antitumor Vaccines Based on Dendritic Cells and B Cells.* Human Gene Therapy, 2010. **21**(12): p. 1697-1706.
74. Brouwer, E., et al., *Human adenovirus type 35 vector for gene therapy of brain cancer: improved transduction and bypass of pre-existing anti-vector immunity in cancer patients.* Cancer Gene Ther, 2007. **14**(2): p. 211-9.
75. McVey, D., et al., *Characterization of human adenovirus 35 and derivation of complex vectors.* Virology Journal, 2010. **7**(1): p. 276.
76. Wu, C., et al., *Generation of a replication-deficient recombinant human adenovirus type 35 vector using bacteria-mediated homologous recombination.* Journal of Virological Methods, 2011. **177**(1): p. 55-63.
77. Arnberg, N., *Adenovirus receptors: implications for tropism, treatment and targeting.* Rev Med Virol, 2009. **19**(3): p. 165-78.
78. Wang, H., et al., *A recombinant adenovirus type 35 fiber knob protein sensitizes lymphoma cells to rituximab therapy.* Blood, 2010. **115**(3): p. 592-600.
79. Adams, W.C., et al., *Adenovirus type-35 vectors block human CD4+ T-cell activation via CD46 ligation.* Proceedings of the National Academy of Sciences, 2011. **108**(18): p. 7499-7504.
80. Gaggar, A., D.M. Shayakhmetov, and A. Lieber, *CD46 is a cellular receptor for group B adenoviruses.* Nat Med, 2003. **9**(11): p. 1408-12.
81. Kanerva, A. and A. Hemminki, *Modified adenoviruses for cancer gene therapy.* Int J Cancer, 2004. **110**(4): p. 475-80.

82. Kang, E. and C.O. Yun, *Current advances in adenovirus nanocomplexes: more specificity and less immunogenicity.* BMB Rep, 2010. **43**(12): p. 781-8.

83. Choi, J.-W., et al., *Evolution of oncolytic adenovirus for cancer treatment.* Advanced Drug Delivery Reviews, 2012. **64**(8): p. 720-729.

84. Yu, L., et al., *Adenovirus type 5 substituted with type 11 or 35 fiber structure increases its infectivity to human cells enabling dual gene transfer in CD46-dependent and -independent manners.* Anticancer Res, 2007. **27**(4B): p. 2311-6.

85. Lee, Y.-S., et al., *An α-GalCer analogue with branched acyl chain enhances protective immune responses in a nasal influenza vaccine.* Vaccine, 2011. **29**(3): p. 417-425.

86. Chae, M.-J., *Antitumor Immunotherapeutical Effect of B cell Vaccine Transduced with Modified Adenoviral vector.* 서울대학교 약학과 석사 졸업논문, 2013. 02

87. Peng, S., et al., *Characterization of HLA-A2-restricted HPV-16 E7-specific CD8(+) T-cell immune responses induced by DNA vaccines in HLA-A2 transgenic mice.* Gene Ther, 2006. **13**(1): p. 67-77.

88. Lee, J.S., et al., *A novel sLRP6E1E2 inhibits canonical Wnt signaling, epithelial-to-mesenchymal transition, and induces mitochondria-dependent apoptosis in lung cancer.* PLoS ONE, 2012. **7**(5): p. e36520.

89. Kim, J., et al., *E1A- and E1B-Double Mutant Replicating Adenovirus Elicits Enhanced Oncolytic and Antitumor Effects.* Human Gene Therapy, 2007. **18**(9): p. 773-786.

90. Lee, Y.S., et al., *The Wnt inhibitor secreted Frizzled-Related Protein 1 (sFRP1) promotes human Th17 differentiation.* Eur J Immunol, 2012. **42**(10): p. 2564-73.

91. Ko, H.J., et al., *Immunogenicity and safety profiles of genetic vaccines*

against human Her-2/neu in cynomolgus monkeys. Gene Therapy, 2008. **15**(20): p. 1351-1360.

92. Murata, K., et al., *Immunization with hepatitis C virus-like particles protects mice from recombinant hepatitis C virus-vaccinia infection.* Proceedings of the National Academy of Sciences, 2003. **100**(11): p. 6753-6758.

93. Shao, H.Y., et al., *Immunoprotectivity of HLA-A2 CTL peptides derived from respiratory syncytial virus fusion protein in HLA-A2 transgenic mouse.* PLoS ONE, 2011. **6**(9): p. e25500.

94. Tan, W.G., et al., *Comparative Analysis of Simian Immunodeficiency Virus Gag-Specific Effector and Memory CD8+ T Cells Induced by Different Adenovirus Vectors.* Journal of Virology, 2012. **87**(3): p. 1359-1372.

95. Tsujimura, A., et al., *Molecular cloning of a murine homologue of membrane cofactor protein (CD46): preferential expression in testicular germ cells.* Biochem J, 1998. **330 (Pt 1)**: p. 163-8.

국문초록

암에 대한 면역 억제적인 환경을 극복함과 동시에 암에 대한 강한 면역반응을 일으킬 때 효과적인 항암 면역 치료가 가능하다. 따라서, 위 연구에서는 암세포에 의해 매개되는 면역억제 기전을 탐색하고, B 세포를 이용한 더욱 효과적인 항암 치료 백신을 개발하고자 하였다. 위의 두 가지 전략은 Part I 과 Part II 에 나누어 서술하였다.

암세포는 다양한 수용성 물질을 분비함으로써 자신의 성장과 전이를 촉진시키는 면역 억제적 환경을 형성한다. 골수성 면역억제 세포(Myeloid derived suppressor cell, MDSC)는 암세포의 분열, 변이, 전이 및 암세포에 대한 숙주의 면역반응을 억제하는 데에 주도적인 역할을 하는 암 환경에서 증가하는 대표적인 세포이다. 골수에서의 myelopoiesis 및 골수 외 환경, 주로 비장에서 일어나는 extramedullary myelopoiesis 에 의해 골수성 면역억제 세포가 생성된다고 알려져 있으나 어떠한 기전으로 골수 및 골수 외 myelopoiesis 가 유도되는지는 아직 잘 밝혀지지 않았다. 본 연구에서는 cytokine array 를 통해 암 환경 내의 비장과 혈청에서 osteopontin 이 유의적으로 증가해 있음을 밝혔으며 암세포가 주로 osteopontin 을 생산하는 소스임을 밝혔다. 암세포에서 osteopontin 을 knock-down 시키거나 중화 항체를 통하여 암세포가 생산하는 osteopontin 을 중화시켰을 경우 암의 성장이 저해되었으며 비장에서의 extramedullary myelopoiesis 또한 감소하였음을 관찰하였다. 더불어 osteopontin 은 비장 유래의 $lineage^{neg}/CD127^{-}/CD117^{+}$ $/Sca1^{-}$(LK cell) 표현형을 갖는 골수성 전구세포의 증식을 증가시켰으며, 골수 유래의 골수성 전구세포의 이동 또한 증가시켰다. 또한 osteopontin 은 골수성 전구세포가 더욱 면역 억제적인 MDSC 로 분화하도록 유도하였다. 위 결과는 osteopontin 이

암 면역환경 조성에 관여하고 있음을 밝혔고 나아가 암 면역억제를 극복할 수 있는 새로운 표적이 될 수 있음을 보여주었다.

암 항원에 대한 강한 면역반응 유도는 임상에서 효과적인 항암 면역치료를 하기 위한 필수적인 요소이다. 면역세포를 이용한 항암치료백신은 항암면역반응을 효과적으로 유도할 수 있는 수단이며 본 연구진은 암 항원을 도입한 변형된 아데노 바이러스인 Ad-k35HM 으로 항원전달 하고 NKT ligand 를 적재한 B 세포를 이용하여 효과적인 항암 치료백신을 구축한 바 있다. 위 B 세포백신은 마우스 모델에서 강력한 세포성, 체액성 항암 면역반응을 유도하였고 결과적으로 암의 성장을 효과적으로 억제하였다. 본 연구에서는 추가적으로 위 B 세포 백신의 다양한 특성에 대한 연구를 진행하였다. 또한 Ad-k35HM 으로 항원전달하고 NKT ligand 를 적재한 B 세포백신은 인간의 HLA-A2 분자를 가진 B6.Cg(CB)-Tg(HLA-A/H2-D)2Enge/Jat mice (AAD mice)에서 HLA-A2 항원결정기 특이적인 세포성 면역반응을 효과적으로 유도하였다. 위 연구로 Ad-k35HM 으로 항원도입한 B 세포백신 임상에서 효과적인 항암치료백신이 될 수 있다는 것을 보여주었다.

주요어: 골수성 면역억제 세포, 골수성 전구세포, B 세포 백신
학번: 2009-30459